



# High-frequency O<sub>2</sub>-CO<sub>2</sub> records reveal intensity of river metabolism and lateral exchange in the Danube Delta

Marie-Sophie Maier<sup>1,2,#</sup>, Bernhard Wehrli<sup>1,2,#</sup>, Cristian R. Teodoru<sup>3,#</sup>

- <sup>1</sup> Department of Surface Waters, Research and Management, Eawag, 6047 Kastanienbaum, Switzerland
- Deparatment of Environmental Systems Science, ETH Zurich, 8092 Zurich, Switzerland
- National Research Development Institute for Marine Geology and Geoecology (GeoEcoMar), Dimitrie Onciu Street 23-25, 024053 Bucharest, Romania
  - # The authors contributed equally to this work

Correspondence to: bernhard.wehrli@env.ethz.ch

15

## Short summary (490chars)

Monitoring stations in the Danube Delta revealed two orders of magnitude difference in the intensity of oxygen and carbon dioxide cycles. Biological processes were more intense in delta channels compared to river reaches and were mainly driven by changes in temperature and cloud cover. Spring floods transferred wetland water to downstream river reaches. The statistical analysis of sensor data provided insights into timing, intensity and type of processes in this complex coastal system.

https://doi.org/10.5194/egusphere-2025-5756 Preprint. Discussion started: 26 November 2025 © Author(s) 2025. CC BY 4.0 License.





#### Abstract

Due to their intense terrestrial-aquatic linkages and intense ecosystem metabolism, many river deltas are aquatic hot spots for carbon dioxide (CO2) emissions to the atmosphere. A patchwork of wetlands, lakes, channels, and river reaches often complicates the analysis of CO<sub>2</sub> sources such as ecosystem respiration or lateral transfer. Sensing techniques offer the opportunity of measuring the paired CO<sub>2</sub>.O<sub>2</sub> concentrations at high temporal resolution for periods from days to months. Such time-series allow quantifying diurnal and seasonal cycles of river metabolism and lateral exchange. This study documents paired O2-CO2 measurements at 15-minute time resolution obtained from deployment of sensor packages in river reaches and channels of the Danube Delta in Romania during a total observation period of three years. We show how to combine results from covariance analysis with insights from averaged 24-hour diurnal cycles. The time series reveal two orders of magnitude variability in daily CO2 fluctuations along the main Danube reaches with typical maxima in the early morning and minima in the afternoon. The amplitude of monthly averaged daily cycles was 2-2.5 times larger in delta channels compared to the river reaches and the parameter for metabolic intensity reacted on average four times more sensitive to changes in water temperature and cloud cover within the delta compared to the main river. Inflow of O2-depleted and CO2-rich wetland water to the downstream river stations was most intense during spring floods with estimated mixing rations of up to 5-20% depending on the station. Stoichiometry of O<sub>2</sub>- CO<sub>2</sub> changes pointed to strong contributions of methane oxidation and/or nitrification in 40% of the analysed summer data, which was also evident from the frequently observed oxygen deficiency. During June-July, a monitored lake system and an adjacent channel showed clear evidence for calcite precipitation and a switch to photosynthetic uptake of HCO3. The study illustrates the benefits of a combining covariance analysis with 24-hours averaging for identifying the timing, intensity and type of processes in river metabolism and lateral exchange.





#### 50 1. Introduction

Over the last decades, the paradigm of river systems as reactors (Cole et al., 2007) replaced a pipe model for carbon and nutrient transfer from land to ocean (Degens et al., 1984). Adding wetlands and inundated areas to river corridors (Abril and Borges, 2019) further improved the analysis of carbon (Zuijdgeest et al., 2016) and oxygen dynamics in rivers (Zurbrügg et al., 2012). Reviews of river metabolism (Hotchkiss et al., 2015) covering the land-ocean aquatic continuum from the headwaters to the coastal zone collected an extensive database of carbon fluxes and transformations for large river systems but available data remain more limited in the heterogeneous environments of the coastal and deltaic zones. Estuaries and their coastal vegetation were recently recognized as an effective global carbon sink (Rosentreter et al., 2023) and the risks from coastal change by erosion, subsidence, sea level change and hydraulic modification (Renaud et al., 2013) call for more detailed analyses of actual carbon dynamics in river deltas.

Compared to smaller streams, the monitoring and analysis of ecosystem metabolism in large river sections faces both advantages and challenges (Bernhardt et al., 2017): wide river sections with large open water areas are not shaded by riparian vegetation which reduces the seasonal effects of leave cover. Furthermore, hydrological changes occur more slowly and with smaller amplitude compared to headwater streams where disturbance regimes may induce abrupt ecosystem change such as the abrasion of productive biofilms (Sabater et al., 2016). On the other hand, dynamic flooding of adjacent wetlands and lateral groundwater exchange in large river corridors may play a more important role for CO<sub>2</sub> emissions than the daily oscillations of in-stream metabolism (Borges et al., 2019), (Marzolf et al., 2022). Wetlands are biogeochemical hotspots with high rates of daily gross primary production (Rabaey et al., 2024). Therefore, estimates of CO<sub>2</sub> concentrations and their potential drivers in lowland rivers (Reiman and Xu, 2019) and river deltas (Huertas et al., 2017) could be improved by high-frequency measurements that allow resolving diel and seasonal cycles of photosynthesis, respiration, and transfer across system boundaries (Battin et al., 2023).

Progress in sensor technology (Rode et al., 2016) now facilitates the autonomous registration of water quality parameters at high frequency over time periods of months. Specifically, wetland connectivity (Maier et al., 2022), the role of seasonal flood pulses (Dalmagro et al., 2018) and differences between daytime and nocturnal emissions (Gomez-Gener et al., 2021) can be monitored by in situ sensors. Covariance analysis of paired O<sub>2</sub> and CO<sub>2</sub> measurements from sensor deployments provides insights into the biological, chemical and physical forcing of aquatic ecosystem processes over time (Vachon et al., 2020). This combination of sensor measurements with statistical analysis has proven highly valuable in recent studies (Rocher-Ros et al., 2025) for identifying drivers of CO<sub>2</sub> dynamics in US rivers (Delvecchia et al., 2023) and in the lower Ganges (Haque et al., 2022), for assessing the balance between river metabolism and CO<sub>2</sub> emissions (Solano et al., 2023), for identifying the contribution of lateral inputs to the carbon budget of rivers (Marzolf et al., 2022), and for calculating the fraction of bicarbonate that supports river photosynthesis (Aho et al., 2021).

This study in the Danube Delta builds on previous analyses of discrete monthly sampling campaigns over the period of two years (Maier et al., 2021) which revealed median CO<sub>2</sub> fluxes in the main branches of the Danube of 25 mmol CO<sub>2</sub> m<sup>-2</sup> d<sup>-1</sup>, and four times higher values in the canals connecting wetlands and lakes. A subsequent onsite mapping study of dissolved gases at high spatial resolution by membrane-inlet mass spectrometry (Maier et al., 2022) revealed hot-spots in emission rates caused by wetland water entering the canal systems, by plant mediated gas transfer via O<sub>2</sub> ebullition in lakes, and by excess air formation in reed stands. Here we report results from a two-year deployment of multiprobe EXO2 sensors recording every 15 minutes in the three main stems of

https://doi.org/10.5194/egusphere-2025-5756 Preprint. Discussion started: 26 November 2025 © Author(s) 2025. CC BY 4.0 License.





the Danube in the Romanian part of the delta near the Black Sea coast which was followed by a one-year deployment in selected channels of the delta. The sensors measured temperature, conductivity, dissolved oxygen and pH. Dissolved CO<sub>2</sub> was calculated from a correlation of conductivity with alkalinity and from the recorded pH and temperature data. The different O<sub>2</sub>-CO<sub>2</sub> time series characterized diverse processes in main river reaches, and in the delta with its reed stands, channels and lakes. To assess the temporal dynamics, we performed covariance analyses of daily and monthly O<sub>2</sub>-CO<sub>2</sub> patterns (Vachon et al., 2020) and calculated mean 24-hour cycles of O<sub>2</sub>-CO<sub>2</sub>. We addressed the questions which potential physical drivers, such as temperature, irradiation, and runoff, govern the variability of dissolved CO<sub>2</sub> and O<sub>2</sub> at daily and monthly time intervals and which biogeochemical processes such as photosynthesis, respiration, methane oxidation or calcite precipitation were shaping the O<sub>2</sub>-CO<sub>2</sub> cycles. On a methodological level, we analysed the merits and limitations of covariance analysis and averaged 24-hour cycles for gaining process-level insights from paired O<sub>2</sub>-CO<sub>2</sub> observations.

## 2. Materials and Methods

## 2.1 Study site and monitoring stations

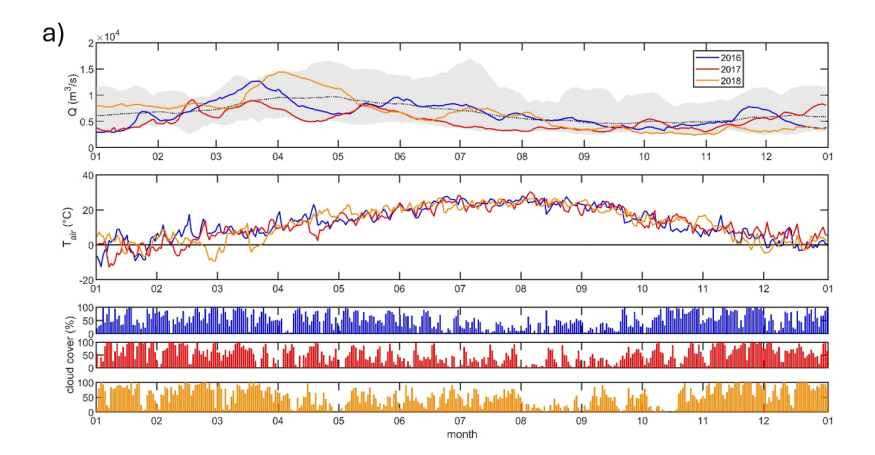
The Danube River is the second largest river in Europe and its international catchment of 817'000 km² covers parts of 19 European countries (Icpdr, 2018). Originating in the Black Forest Mountains in Germany, the Danube flows southeast for over 2'857 km before discharging into the Black Sea. The annual average flow rate is 6360 m³ s⁻¹ and ranged from 2'930 m³ s⁻¹ to 11'300 m³ s⁻¹ in the period 1921-2015 at the Ukrainian station of Reni (Romanova et al., 2019). Receiving meltwater from the Alps and the Carpathian Mountains, the hydrology of the Danube River has a pronounced seasonality. In general, peak discharge lasts from April to June and low flow conditions prevail between September and November. A secondary maximum in discharge usually occurs from December through January due to rainfall in the lower catchment (Fig. 1a). Seasonal temperature changes varied from around zero °C in winter to 20-25°C in summer. The probability of cloud cover was higher in winter than in summer.

Close to the mouth, the river splits into three arms that form the Danube Delta: Chilia in the north constitutes the border with Ukraine, Sulina in the middle was modified for maritime commercial navigation while Sfantu Gheorghe (St. George) limits the delta area in the south (Fig. 1b). The surface area of the Danube Delta between these river reaches is approximately 4150 km², of which more than 80% is part of Romanian territory. As the youngest and the longest among the three arms, the 120 km long Chilia branch carries more than 50% of the Danube water, the 64 km long Sulina channel about 27% and the 70 km long river reach of St. George contributes about 20% to the total water discharge into the Black Sea. Travel-time analysis based on our sensor data resulted in average flow velocities in the range of 0.7-1.0 m s<sup>-1</sup>.

An intricate network of lakes, swamps, shallow water pools and channels connects the delta's wetlands with the river. Although considered the most pristine delta in Europe, a series of hydrotechnical works in the Danube Delta, mostly for agriculture and fishery, lead to doubling the length of the internal canals after 1980 (Gatescu et al., 1983). This, in turn, gradually increased the water flow through the delta from 260 m³ s⁻¹ between 1951 and 1960 to 620 m³ s⁻¹ in the period 1981-1990 (Bondar, 1994). Today, approximately 10% of the total Danube discharge is considered to enter the delta, of which about 20% (120 m³ s⁻¹) may be lost via evapotranspiration in the wetland and its reed stands (Oosterberg et al., 2000).







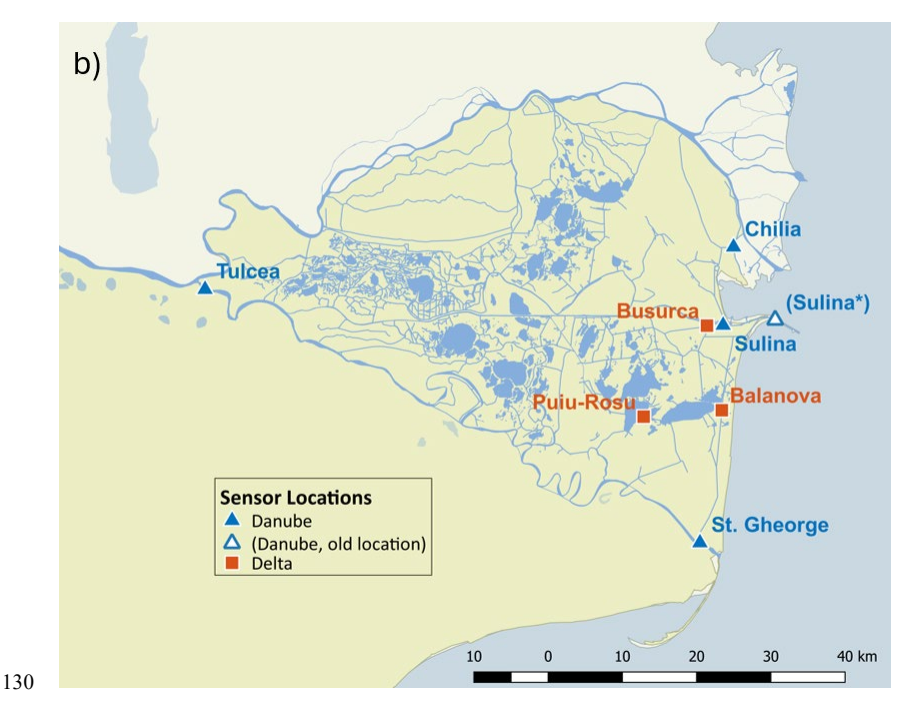


Figure 1a) – Three years of environmental records for the Danube Delta 2016-2018. Top: average daily discharge of the Danube at Reni, Ukraine, upstream of the Delta (available at https://www.danubehis.org/stations - last access 27. Oct. 2025). Gray area shows the range of daily discharge for the period 1998-2017. Middle: average daily air temperature; bottom: average daily cloud cover at Tulcea Airport (available at https://rp5.lv/Weather\_in\_Tulcea\_(airport) – last access 27. Oct. 2025). b) Monitoring locations for EXO2 probes in main branches and within the Danube Delta, the old location refers to Sulina station in 2016, which was relocated in 2017. Map: © OpenStreetMap contributors 2024. Distributed under the Open Data Commons Open Database License (ODbL) v1.0.





In the first phase of this study, we deployed four sensor packages (EXO2 Multiparameter Water Quality Sondes, YSI) in the main branches of the Danube River at the stations labelled Tulcea, Chilia, Sulina, and St. George (Fig. 1a). The monitoring stations recorded data every 15 minutes between November 2015 and February 2018 (Fig. A1, Table A1). One multiprobe was damaged by the floating ice in December 2016 which shortened the time series at Chilia station. In the second phase from February 2018 to December 2018, the remaining three EXO2 probes were installed in channels within the delta at stations Balanova, Busurca and Puiu-Rosu. Note that Balanova is a local name for a site on the Central Channel that connects the Sulina and St. George branches (Fig. 1b).

## 2.2 Measured and derived parameters

The EXO2 multiprobe sensors recorded temperature, pH, specific conductivity, and dissolved oxygen every 15 minutes. The output of additional sensors for turbidity and fluorescent dissolved organic matter (fDOM) were not analyzed for this study. Before each measurement, the individual sensor caps were cleaned automatically by a wiper. The EXO sensors were moored at approximately 1 m below the water surface. Data gaps in the time series occurred sporadically due to unexplained energy drain from batteries and when probes were removed to prevent damage by floating ice sheets during cold spells in winter. Once a month, the probes were removed from the water and cleaned and pH and O<sub>2</sub> sensors were calibrated using standard solution and air-saturated water, respectively. Post-deployment, the data was drift-corrected using the calibration data. Crosschecks with discrete in situ measurements using the YSI Optical Dissolved Oxygen and Professional Plus Multiparameter sensors (Maier et al., 2021) showed good agreement. We used a low conductivity threshold (< 200 μS cm<sup>-1</sup>) to detect and delete invalid data points measured at times when the sensor was out of the water for servicing.

We derived the alkalinity time series from specific conductivity data using the linear correlation (Maier et al., 2021) between laboratory analysis of alkalinity and specific conductivity measurement as: alkalinity (mmol  $L^{-1}$ ) = 0.0057\*SpCond (µS cm<sup>-1</sup>) + 0.60, Fig. B1). To calculate CO<sub>2</sub> from pH and alkalinity, we used the CO2SYS MATLAB code version 1.1 with Matlab R2017a and 2022b (Van Heuven et al., 2011). These calculations were 165 based on the dissociation constants from (Cai and Wang, 1998) for a temperature range of 2°C to 35°C and a salinity from 0 to 49 %. To obtain an upper and lower estimate for the derived CO<sub>2</sub> time-series, we propagated the uncertainty related to the alkalinity-conductivity regression estimates and obtained an error of  $\pm$  13%. The calculated CO2 values correlated well with discrete headspace measurements taken at the same time and location (Fig. B1). Finally, we used solubilities (Weiss, 1974) and the temperature recordings from the EXO2 probes to 170 calculate the deviation from atmospheric equilibrium in µmol L-1 of the O<sub>2</sub>-CO<sub>2</sub> pairs. We defined the frequent excess of CO2 and the typical deficit of O2 with regards to atmospheric equilibrium as exCO2 and exO2 with a positive or negative sign, respectively, and we determined the dissolved concentrations in the µM range. For the correlation of this O<sub>2</sub>-CO<sub>2</sub> time series with meteorological and hydrological conditions we used hourly data from a meteorological station in Tulcea covering the years 2015-2019 (Fig. 1a). The time-shift of one hour during daylight saving time was removed to synchronize the data with the continuous recording of EXO probes. Daily averages of air temperature and cloud cover as a proxy for reduced irradiation were used as potential physical drivers for river metabolism and water levels at Tulcea were tested as potential drivers for lateral exchange between wetland and river system.

Some data-cleanup was necessary for the time series of Chilia (2016) and Sulina (2017) which were sporadically influenced by water from an adjacent wetland and from the Black Sea, respectively, which lead to steep increases

https://doi.org/10.5194/egusphere-2025-5756 Preprint. Discussion started: 26 November 2025 © Author(s) 2025. CC BY 4.0 License.





in specific conductivity (spike events). We flagged these points as spikes by comparing the time series with upstream Tulcea station and if the data deviated more than  $40~\mu S~cm^{-1}$  from the baseline. This approach missed the beginning and the end of the spike events. To refine the cleanup, we took 5 hours before and after an identified spike event and eliminated periods with changes in specific conductivity larger than  $2~\mu S~cm^{-1}$  and completed the task with few manual adjustments.

#### 2.3 Statistical analysis

Vachon et al. (2020) proposed a set of parameters obtained from covariance analysis of paired  $O_2$ - $CO_2$  measurements to gain insights into aquatic ecosystem metabolism. We implemented this approach with Mathematica 14.0 to analyze the Danube Delta time series at monthly and daily timescales. Days with less than 85 data pairs were excluded from analyses, as typically 96 pairs were recorded daily at 15 minutes intervals. Monthly analyses usually involved more than 2800 pairs and datasets with less than 500 pairs were excluded from further analysis. The centroids represent the mean of the  $exO_2$  and  $exCO_2$  data over the period of days or months. Stretch and width were obtained from the Eigenvalues of the covariance matrix as the major and minor axes length of the 95% error ellipse (Fig. 2a). As an extension to the proposal of Vachon et al. (20220), we defined a negative sign for the offset if the centroid was located below the 1:-1 line (Fig. C1). We obtained the slope  $s_{cov}$  of the stretch-line from the Eigenvectors of the covariance matrix. The Eigenvector approach worked even for almost circular patterns with a stretch to width ratio < 4.0, when a reduced mean axis (RMA) regression algorithm failed to converge.

Parameters obtained from covariance analysis provide valuable insights into the intensity of photosynthesis and respiration (stretch), the ecosystem quotient (EQ = 1/slope), and the impact of confounding processes such as lateral inflows or microbial processes (centroid, offset). These confounding processes often obscure the dynamics of photosynthesis and respiration at monthly timescales. To analyse monthly day-night dynamics, we calculated the average 24 hours day-night cycles for each month of sensor deployment. This approach resulted in average timing and amplitude of daily O<sub>2</sub>-CO<sub>2</sub> cycles. These time-of-day averages reduced the weight of outliers and resulted in slopes s<sub>24</sub> that reflect EQs more closely than the tilt of the covariance ellipse (s<sub>cov</sub>) which is co-defined by lateral inflows (Fig. 2b). Comparing the 105 available monthly records showed that s<sub>24</sub> slopes from 24-h monthly averages were in general steeper than s<sub>cov</sub>. The median ratio of s<sub>24</sub>: s<sub>cov</sub> was 1.56 (Fig. C2).



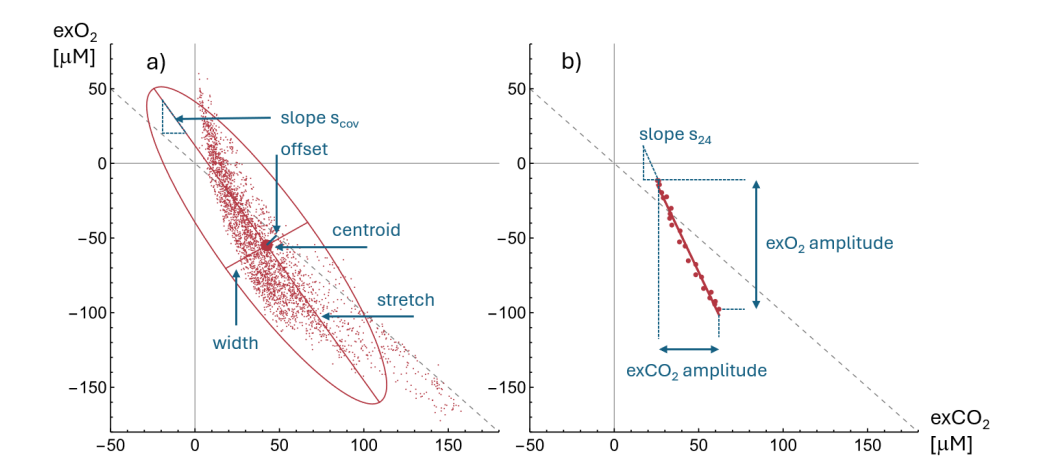


Figure 2 a) Example of covariance analysis of exCO<sub>2</sub>-exO<sub>2</sub> data from July 2018 at Balanova station. Smal dots are individual data points acquired every 15 minutes, the large dot marks the centroid, i.e. the mean exCO<sub>2</sub> and exO<sub>2</sub> concentration of the month. The ellipse encloses 95% of the datapoints and is constructed with the centroid and the two main axes (125 and 29 μM) calculated from the Eigenvalues of the covariance matrix. The covariance slope s<sub>cov</sub> (-1.56) is calculated from the Eigenvector of the covariance matrix. The offset is calculated as the nearest distance of the centroid from the grey dotted line with -1 slope for a theoretical photosynthesis-respiration metabolism. b) Using the same data as in a), the monthly averages over 24 hours of the day define a mean daily cycle for July at Balanova station. The 24-h slope s<sub>24</sub> in this example is – 2.4. The average daily cycle shows an exCO<sub>2</sub> amplitude of 36 μM but a wider exO<sub>2</sub> amplitude of 88 μM with a maximum oxygen deficit at 6:30 AM and an exO<sub>2</sub> maximum at 4:30 PM (compare Fig. 3).

#### 3. Results

220

225

# 3.1 Daily fluctuations of carbon dioxide and oxygen

The lower Danube shows consistent oversaturation with respect to  $CO_2$  and significant oxygen deficits compared to atmospheric equilibrium. To provide an overview of the  $exCO_2$  and  $exO_2$  dynamics in the Danube and its delta, at both seasonal and daily timescales, we calculated the monthly averaged diel fluctuations (Fig. 3, Fig. D1). Before splitting into three branches that confine the area of the delta, the Danube River at Tulcea station shows only a small and constant supersaturation ( $exCO_2$ ) and undersaturation (negative  $exC_2$ ) over day-night cycles and seasons. Deviations from equilibrium concentrations were mostly confined to +-  $20-40 \mu M$ . Exceptions occurred in June 2016 and from May to June 2017, when  $O_2$  was oscillating with a low average amplitude of 6-9  $\mu M$  close to equilibrium, which was an indication for in-stream photosynthesis (Table 1). The downstream locations of Sulina (2016) and St. George showed strong  $CO_2$  supersaturation with concentrations increasing from summer to autumn (Fig. D1). During the warm season,  $exC_2$  in St. George and Chilia were marked by significant diel cycles of 20-30  $\mu M$ . These strong differences in the level and daily amplitude of  $CO_2$  and  $O_2$  building up in the  $\sim 60$  to





120 km of river flow from Tulcea to the three near-shore stations indicated important inflows from the Danube Delta wetlands at these stations.

The observations within the Delta in 2018 provide information on typical concentration ranges of CO<sub>2</sub> and O<sub>2</sub> in these lateral inflows. While the concentrations in the winter months remained close to the values of Tulcea, the CO<sub>2</sub> curves show strong daily oscillations. For consistency, the timing is clocked by Easter European Time (EET) without a shift to summertime (EEST). Dynamics at the Balanova station was characterized by maxima in the early morning (6-8 AM) and minima in the afternoon (4-6 PM) between April and November (Fig. 3). Compared to CO<sub>2</sub>, the oxygen curves represented a mirror image where the strong undersaturation in the morning hours relaxed to equilibrium values in the late afternoon. The amplitude of these average daily oscillations reached maxima of 49 and 104 μM for exCO<sub>2</sub> and exO<sub>2</sub>, respectively (Table 1). By contrast, the outflow of the lake complex Puiu-Rosu was closer to atmospheric equilibrium (Fig. D1) and had smaller exCO<sub>2</sub> concentrations and daily amplitudes up to 19 μM. Also, exO<sub>2</sub> from the lake complex showed oscillations occurring close to equilibrium but with amplitudes like Balanova (up to 108 μM). The Busurca Channel represented an extreme case because it drains significant amounts of wetland water. As a result, the monthly average of the daily patterns showed CO<sub>2</sub> levels around 300 μM in February-March and reached almost 500 μM in May and July, when the O<sub>2</sub> concentrations approached anoxic conditions

Overall Table 1 reveals two orders of magnitude difference in daily metabolic cycles between the upstream station of Tulcea in winter and the Balanova channel in summer. Averaging the annual data resulted in 6 µM exCO<sub>2</sub> and 11 µM exO<sub>2</sub> for the four Danube River stations and 18 exCO<sub>2</sub> and 43 µM exO<sub>2</sub> for the three delta stations. Compared to the river reaches, the metabolic shifts at the monthly timescale were therefore 2-2.5 times more intense within the delta water network. The average amplitudes during the warm season of April to September were about 40% larger than the annual mean values.

**Table 1.** Amplitude of average daily fluctuations (Fig. D1) in  $exCO_2$  and  $exO_2$  in  $\mu M$  at four Danube stations in 2016 and at three stations within the delta in 2018. The av. column shows the annual average of available data.

		av.	Jan	Feb	Mar	Apr	May	Jun	Jul	Aug	Sep	Oct	Nov	Dec
Tulcea	$exCO_2 \\$	1				0.3	0.5	2	2	2	3	1	0.4	0.8
	$exO_2$	5				2	4	8	8	6	9	3	0.7	1
Sulina	exCO <sub>2</sub>	3				3	3	7	6	2	3	3	2	1
	$exO_2$	4				6	6	8	6	4	2	1	1	1
St. George	exCO <sub>2</sub>	15	4	8	15	17	19	29	25	12	16	8	8	
	$exO_2$	21	8	15	29	32	25	30	31	23	30	4	7	
Chilia	exCO <sub>2</sub>	5	2	2	2	2	2	3	8	10	10	15	5	1
	$exO_2$	12	8	5	3	7	11	12	20	23	28	13	4	4
Balanova	exCO <sub>2</sub>	24		5	2	12	25	41	37	49	48	22	23	4
	$exO_2$	52		9	12	35	59	95	86	104	78	50	29	14
Puiu-Rosu	exCO <sub>2</sub>	8		3	3	7	8	7	14	19	8	8	6	9
	$exO_2$	47		11	12	28	23	68	90	108	84	50	27	20
Busurca	exCO <sub>2</sub>	23		15	14	30	12	23	37	53	34	16	5	11
	$exO_2$	30		13	21	42	29	47	29	58	50	21	4	15





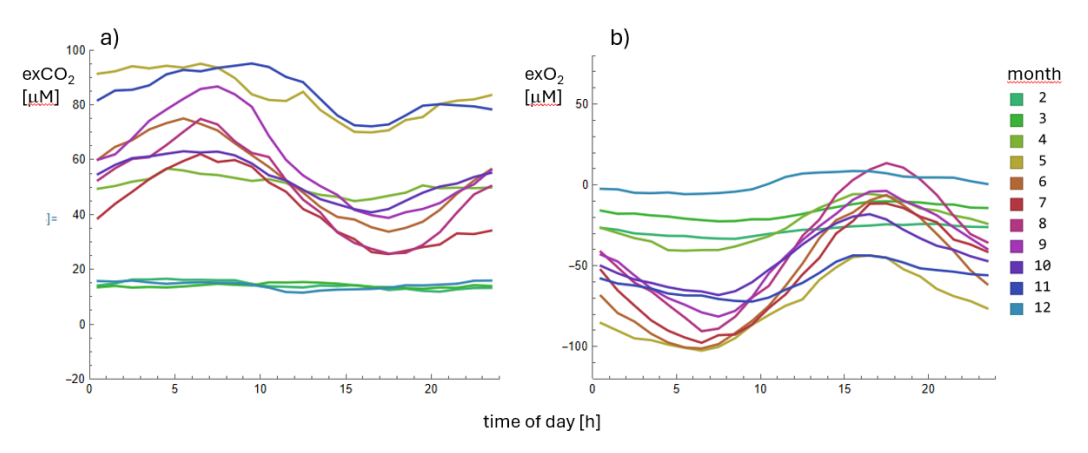


Figure 3. Example of 24-h monthly averages for a)  $\exp(O_2)$  and b)  $\exp(O_2)$  at Balanova station in 2018. Time-of day on x-axis, excess  $ext{CO}_2$  and  $ext{O}_2$  on y-axis, color-coding shown at right. The averaged daily cycles define characteristic amplitudes and timing of river metabolism during each month. For full data see Fig. D1.

265

## 3.2 Covariance of O2-CO2 dynamics

In an ideal case, aquatic photosynthesis and respiration represent the major drivers for change in dissolved O<sub>2</sub> and CO<sub>2</sub> concentrations in surface waters. A plot of exO<sub>2</sub> versus exCO<sub>2</sub> would then resemble a straight line with slope -1 crossing zero excess concentration (Vachon et al., 2020). At the delta stations, inflow from the wetlands and 270 variable biogeochemical processes variability define broader domains of observed exCO2-exO2 values and associated covariance parameters (Fig. 4). We calculated covariance data from a set of 105 monthly observations (Table D1). As expected, there were strong correlations (Pearsons's  $\rho > 0.5$ ) between the centroid CO<sub>2</sub> and O<sub>2</sub> position and the offset from the -1 line and between stretch and width, the long and short axis of the 95% ellipses (Table 2). There was weaker correlation between the centroid position and the shape parameters of the ellipses. 275 The slope, which should relate to the ecosystem stoichiometry, showed the weakest correlations with other parameters, indicating that the intensity of river metabolism (stretch) was quite independent of the type of processes (slope). In November 2016, the centroid coordinates at stations Tulcea, Sulina and Chilia were located close to the theoretical line in the lower right segment, i.e. in the respiratory domain of the O2-CO2 plot with exCO2 > 40 and exO<sub>2</sub> around -35 μM (Fig. 4, Table D1). The over 2500 datapoints in November were confined to quite narrow covariance ellipses enclosing 95% of the datapoints measured within one month. At St. Geroge, however, the November data were spreading over a much larger area ( $\sim 50 < \text{exCO}_2 < 150 \,\mu\text{M}$ , centred around enriched exCO<sub>2</sub> =102  $\mu$ M and more depleted exO<sub>2</sub> = -47  $\mu$ M). The offset of the centre is defined as the nearest distance to the 1:-1 line and reached a value of 28 μM at St. George in November compared to a range of 4-8 μM at the other three 285 Danube stations. This increased offset towards high CO2 is a strong indication for lateral inflow from the reed stands in the wetland, where the decomposition of organic matter accumulates dissolved CO2.





**Table 2** Correlation coefficients  $\rho$  for 105 monthly parameter sets including the centroid position (c-exCO<sub>2</sub>, c-290 exO<sub>2</sub>), the shape parameters stretch and width, the offset, and the slope of the main ellipse axis (Data in Table D1). Bold face for  $|\rho| > 0.5$  and grey font for  $|\rho| < 0.2$ .

parameter	c-exCO <sub>2</sub>	c-exO <sub>2</sub>	stretch	width	offset	slope
c-exCO <sub>2</sub>	1					
c-exO <sub>2</sub>	-0.93	1				
stretch	0.46	-0.38	1			
width	0.49	-0.45	0.74	1		
offset	0.92	-0.75	0.45	0.43	1	
slope	0.13	-0.14	-0.08	0.02	0.09	1

In the covariance data from June 2016, the inflow of water from the Delta wetlands is leaving its marks in all three downstream stations of the Danube (Fig. 4). The covariance ellipses show an elongated shape due to more intense photosynthesis and respiration compared to November, but the quite uniform distribution of measurements within the ellipses at St. George and Chilia corresponds to strong day-night shifts, while the "random walk" of datapoints in the exCO<sub>2</sub>-exO<sub>2</sub> domain of Tulcea and Sulina in Fig. 4 corresponds to significantly smaller amplitudes of the daily fluctuations (Table 1). Note that the oxygen dynamics at Tulcea was centred around atmospheric equilibrium in June, but in the context of the full year, this represents an exception. Usually, Tulcea waters showed slight oxygen deficits.

The observations within the Danube Delta in 2018 reveal a striking difference to the main reaches of the Danube: In June, the covariance in the CO<sub>2</sub>-O<sub>2</sub> plain is constrained by narrow 95%-ellipses and the three sites widely differ in the slope of the main axis of -1.6, -7.8 and -0.3, for Balanova, Puiu-Rosu and Busurca, respectively. This contrast and the distinctive average exO<sub>2</sub> values (-58, +19, -206 μM) at these three sites point towards different governing processes (Table D1). Compared to the covariance analyses in the main stem of the Danube, the two sites at Balanova and Puiu-Rosu exhibit only negligible offsets while Busurca's offset in June with > 100 μM marks only one of several excursions towards high exCO<sub>2</sub> at that site. The Puiu-Rosu station seems therefore to be dominated by aquatic processes characteristics for lakes, whereas Busurca and Balanova, which collect the outflow from the wetlands, show a mixture of both sources.



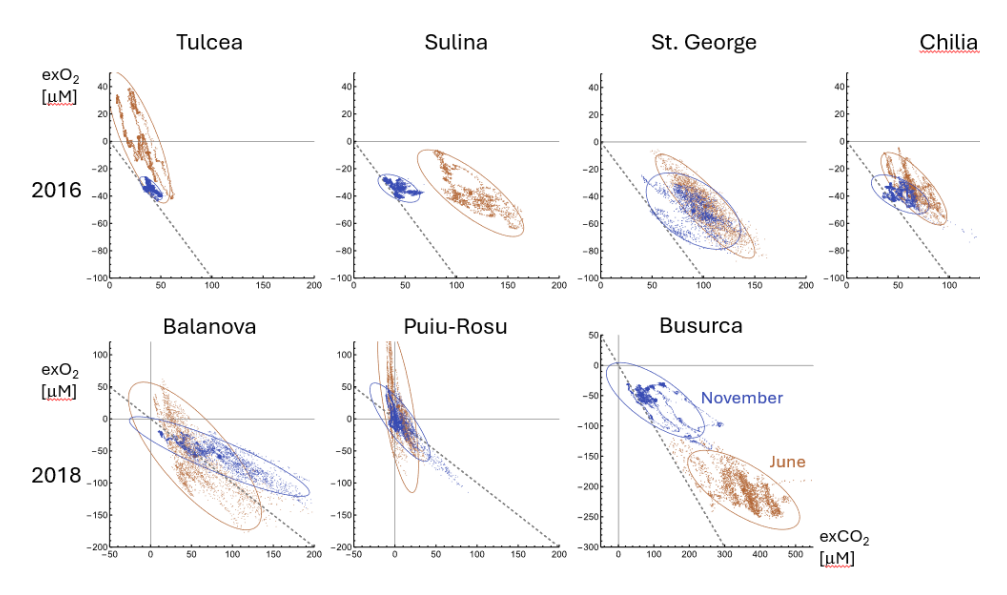


Figure 4. Examples of covariance ellipses for  $exO_2$  vs.  $exCO_2$  covering 95% of measured data pairs for the Danube River reaches and stations within the delta. The diagonal line represents the theoretical slope of -1 crossing the origin. Top: months June (red) and November 2016 (blue) for the four Danube River stations. Bottom: June (red) and November 2018 (blue) at stations within the delta, the Balanova station, the outflow from Lake Puiu and the station Busurca at the channel collecting outflow from the reed stands.

## 4. Discussion

320

325

## 4.1 Lateral inflow from wetlands

In the absence of lateral inflow, one would expect very similar chemical characteristics among the Danube stations of Tulcea upstream of the Delta and the three sites of St. George, Sulina and Chilia close to the Black Sea. The data clouds, however, revealed clear differences in exO2-exCO2 between Tulcea and the stations downstream (Fig. 4). A more systematic analysis of the centroids allows tracking how the monthly means of exO2-exCO2 move over time. The results reveal quite diverse annual journeys at the four Danube stations in 2016 and 2017 (Fig. 5). The trajectories at Tulcea were confined to a quite narrow quadrant between 0 and  $\pm$  40  $\mu M$  for exO<sub>2</sub> and exCO<sub>2</sub>. At the downstream stations, however, the centroids for summer and autumn typically fall outside this range because waters were loaded with excess CO<sub>2</sub> and more depleted in O<sub>2</sub> compared to Tulcea. The increase in average exCO<sub>2</sub> between Tulcea and a downstream station reached factors of 4 (June 2016, Sulina) and 18 (June 2017, St. George). Both stations were influenced by canals draining the delta and therefore partially reflect mixing of Danube waters with lateral inflows from the wetlands and their groundwater. Recently (Deirmendjian and Abril, 2018) reported such groundwater hotspots in first-order streams. The downstream depletion of exO2 at Sulina and St. George was less pronounced than exCO2 loading and maximum exO2-differences compared to Tulcea were limited to a factor of ~ 3 (Sulina, July 2017) and 2 (St. George, Oct. 2016). In streams, the mineralization of organic matter changes dissolved CO2 and O2 with a 1:1 stoichiometry, but in groundwaters and wetland outflows the oxygen can be depleted to near-zero concentrations, while the accumulation of dissolved CO2 continues by anaerobic processes





and may reach very high levels (Maier et al., 2022). The different hydrographs in 2016 and 2017 lead to distinct excursions in CO<sub>2</sub> loads at Sulina and St. George. While the recession of the spring flood coincided with an input of exCO<sub>2</sub> in June at the Tulcea branch, the very low water levels in summer 2017 (Fig. 1a) drained exCO<sub>2</sub> rich water specifically into the St. George Branch (Fig. 5). By contrast, the Chilia station, mostly recorded Danube water signatures and showed only moderate deviations from the centroid dynamics at Tulcea.

340 The largest flood peak in the three years of our study occurred in early April 2018. It was followed by a strong flood recession until mid-June. All three stations in the Delta showed the highest CO2 loads and the lowest O2 levels in May 2018, when the flooded reed stands were likely exporting water into the channels and lakes. Higher discharge in July-August lead to a reversed situation, but then exceptionally dry conditions kicked in and even the Busurca Channel seemed to be carrying mostly Danube water in December 2018 (Fig. 5). Within the delta, the Balanova station in 2018 provides an illustrative example of in-stream metabolism dominated by mineralization of organic matter generated in the wetlands of the delta (Maier et al., 2022). During summer, the centroids remained in the domain of oxygen deficits but follow the 1:-1 stoichiometry quite closely (Fig. 5). The Busurca Channel, however, represents an endmember collecting mainly waters from the wetland, with a pattern strongly deviating from the stoichiometry of river metabolism and average oxygen levels approaching anoxic conditions with close to -250 µM exO<sub>2</sub> in spring and summer and dissolved CO<sub>2</sub> concentrations exceeding a 30-fold oversaturation (470 μM exCO<sub>2</sub>) in May and June. Such a water composition of almost 500 μM exCO<sub>2</sub> could be defined as an observed endmember in the water composition of the wetlands. In such a scenario, maximum excursions with maximum offsets of 20 µM at Chilia (June 2016), 54 µM in Sulina (June 2016) and of 116 µM at St. George (June 2017, Table D1) would correspond to mixtures of Danube water with ~4, ~10 and ~25% CO<sub>2</sub>- rich wetland water, 355 respectively.

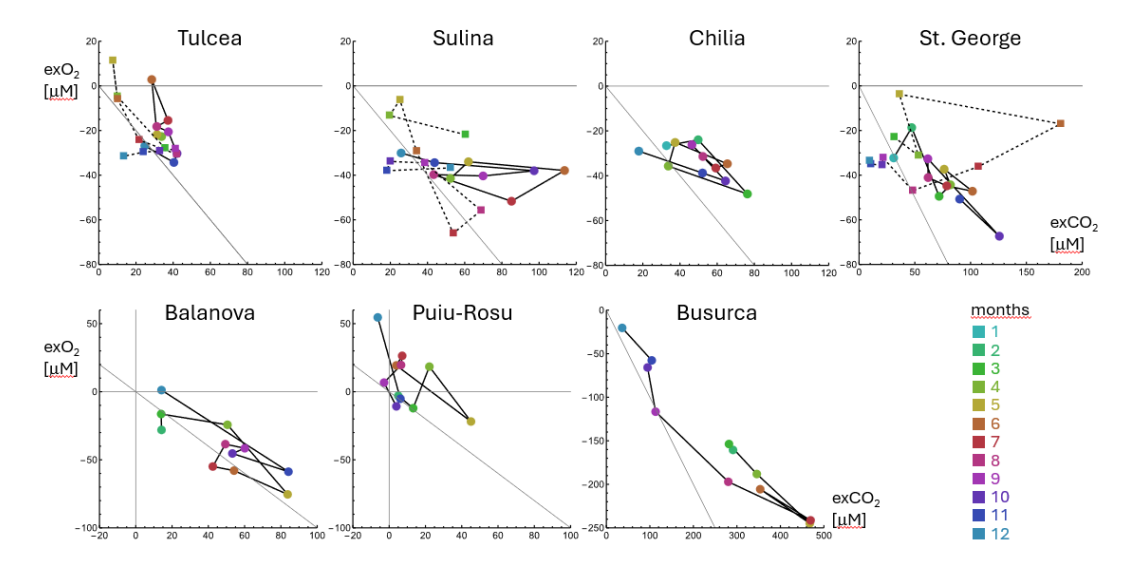


Figure 5. Top: Annual trajectories of monthly centroids at the four Danube River stations in 2016 (dots connected by solid lines) and 2017 (squares connected by dotted lines). Note different x-axis for St. George. Bottom: Monthly centroids at three stations within the Danube Delta in 2018 (dots with black lines). Note different axes for Busurca.

https://doi.org/10.5194/egusphere-2025-5756 Preprint. Discussion started: 26 November 2025 © Author(s) 2025. CC BY 4.0 License.





These estimates are plausible, given that an average 10% of the Danube water passes through the delta (Bondar, 1994) and the wetland outflow near the monitoring stations of Sulina and St. George was incompletely mixed with river water.

365 The Puiu-Rosu station was dominated by the outflow of Lake Puiu and provides a contrasting example of average exO<sub>2</sub> dominated by photosynthesis and very low or even negative exCO<sub>2</sub> due to uptake by algae and macrophytes. Here, the highest CO<sub>2</sub> levels were observed in May which is consistent with the other two stations at Balanova and Busurca. The probable driver for inputs of CO<sub>2</sub>-rich water was a flood recession in response to the extreme flood peak in April 2018 (Fig. 1a). During summer, the centroids of Puiu-Rosu cluster around equilibrium values of CO<sub>2</sub> and oversaturation with respect to atmospheric oxygen.

## 4.2. Flooding and flood recession

While tracking monthly centroids helps detecting lateral inflows at monthly to seasonal timescales, we need a finer time-resolution to test hypotheses regarding the drivers for lateral exchange. For this study, daily water level records at Tulcea were available as flow proxies (Fig. 1a). Therefore, we tested the hypothesis that floods would push water into the wetlands, which would then carry high CO<sub>2</sub> water with O<sub>2</sub> deficits back into the delta's channel network when water levels decreased. Time-delay analysis of peak conductivity and turbidity at Tulcea compared to the downstream stations revealed flow times of approximately 1 day from Tulcea to Sulina and 2 days to Chilia and St. George. Based on published work, we assumed typical delay times of 20 days to Puiu-Rosu and 40 days to Balanova (Oosterberg et al., 2000), but these travel times may vary and the estimates are therefore poorly constrained. We excluded three data sets with significant gaps from the analysis: Chilia 2016, Sulina 2017 and Busurca 2018.

As expected, the coefficients ρ of exCO<sub>2</sub> had opposite sign compared to exO<sub>2</sub>, however, correlations between daily covariance parameters and time-shifted Tulcea water-levels revealed some puzzling results (Table 3): the shape parameters (stretch and width) and the offset had different signs on the correlation coefficient ρ at St. George in 2016 compared to 2017. In 2016, the daily exCO<sub>2</sub> centroids were positively correlated with water levels indicating a trend that flooding was pushing CO<sub>2</sub>-rich wetland water towards the monitoring station, while the weak negative correlation in 2017 points toward the role of flood recession in building up the large exCO<sub>2</sub> observed at minimal discharge values in June (Fig. 5). These contrasting correlations indicate that upstream daily flood levels alone cannot predict the transfer of CO<sub>2</sub> and O<sub>2</sub> from wetlands to river reaches. The timing of discharge peaks and minima in relation to the seasonal CO<sub>2</sub>-O<sub>2</sub> dynamics in the wetlands seems to play a significant role in the covariance analysis of annual data.

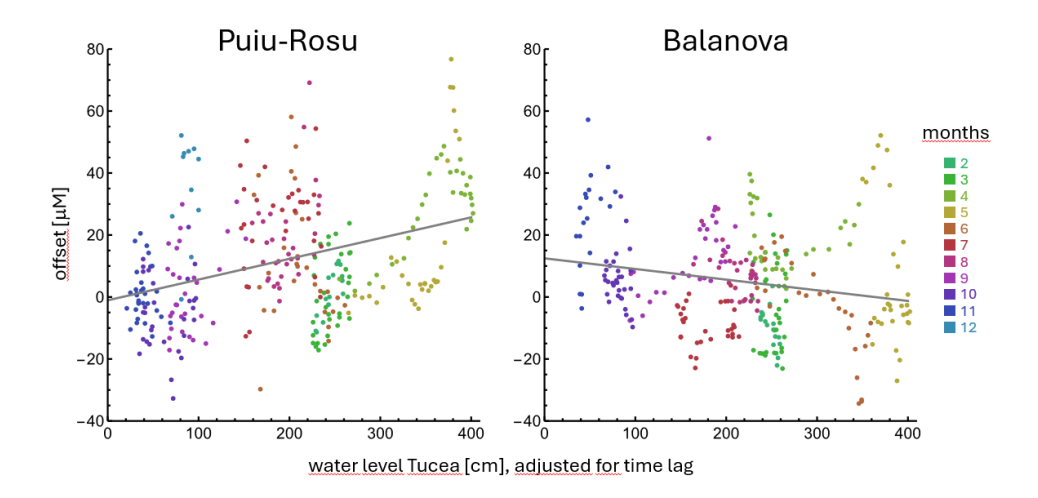
A comparison of the correlation between offset and time-adjusted water levels in Tulcea for two time series of Puiu-Rosu and Balanova illustrates this critical relationship between aquatic metabolism and the dynamics of flooding and flood recession (Fig. 6). The lake ecosystem of Puiu-Rosu remained close to the -1 line in autumn so that the high-CO<sub>2</sub> flood pulse in spring determined the slope of the linear regression. By contrast, the wetland dominated Balanova Channel received significant CO<sub>2</sub> inputs when low water levels were draining the reed stands in autumn. We can therefore reject the simple hypothesis that upstream water levels of the Danube could predict daily CO<sub>2</sub>-O<sub>2</sub> dynamics within the delta. Local water-level measurements are needed for a meaningful analysis. The "annual journey of centroids" in Fig. 5, however, provides a valuable basis for qualitative assessments of lateral inflows and their contributions to exO<sub>2</sub>-exCO<sub>2</sub> dynamics at monthly to seasonal time scales.





**Table 3.** Daily covariance analysis of seven continuous timeseries of  $exCO_2$  and  $exO_2$  data at five stations. The data were correlated with time-adjusted water level measurements at Tulcea. The Chilia, Busurca and Tulcea 2017 results were omitted due to irregular data gaps. Bold face for  $|\rho| > 0.5$  and grey font for  $|\rho| < 0.2$ 

time-series	delay [d]	c-exCO <sub>2</sub>	c-exO <sub>2</sub>	stretch	width	slope	offset
Tulcea 2016	0	-0.06	0.38	0.16	0.18	0.04	0.43
Tulcea 2017	0	-0.27	0.23	-0.29	-0.42	-0.07	0.06
Sulina 2016	1	0.17	-0.17	0.24	0.41	-0.08	0.13
St.George 2016	2	0.55	-0.39	0.42	0.29	0.07	0.42
St.George 2017	2	-0.15	0.40	-0.26	-0.26	-0.11	-0.02
Puiu-Rosu 2018	20	0.58	-0.04	-0.19	0.29	0.00	0.36
Balanova 2018	40	-0.08	-0.07	0.02	0.21	-0.08	-0.20



415 **Figure 6.** Linear regression between time-adjusted Danube water levels at Tulcea and daily offset at Puiu-Rosu and Balanova in 2018. Time lag at Puiu-Rosu and Blanova was 20 and 40 days respectively.





#### 4.3 Intensity of river metabolism

While the annual trajectories in CO<sub>2</sub>-O<sub>2</sub> space reflect the dynamics of lateral inflows, a closer look at diurnal cycles helps comparing the intensities of autotrophic versus heterotrophic ecosystem metabolism. For a quantitative analysis, we re-plotted the 24-h monthly averages at one hour resolution (Fig. 7). These graphs illustrate the minimal metabolic activity during winter months and comparatively small signals of river metabolism during the summer months for Tulcea and Sulina with some addition of wetland CO<sub>2</sub> downstream at Sulina. St. George and Chilia, however, were characterized by strong daily cycles in exO<sub>2</sub> in a background of CO<sub>2</sub>-rich wetland water.

Within the delta, Balanova represented an example of intense metabolic activity with exO<sub>2</sub> amplitudes up to 100 μM (Table 1). While Puiu-Rosu showed the same intensity, this lake environment represented a case where autotrophic activity significantly exceeded heterotrophic metabolism with positive values of daytime exO<sub>2</sub> during most of spring and summer and even undersaturation of CO<sub>2</sub> in September. By contrast, from April to August Busurca station is completely dominated by wetland waters and exhibited similar day-night dynamics as Balanova, but the oxygen dynamics was significantly smaller due to heterotrophic and methanotrophic activity: in May and July, Busurca station approached complete anoxia.

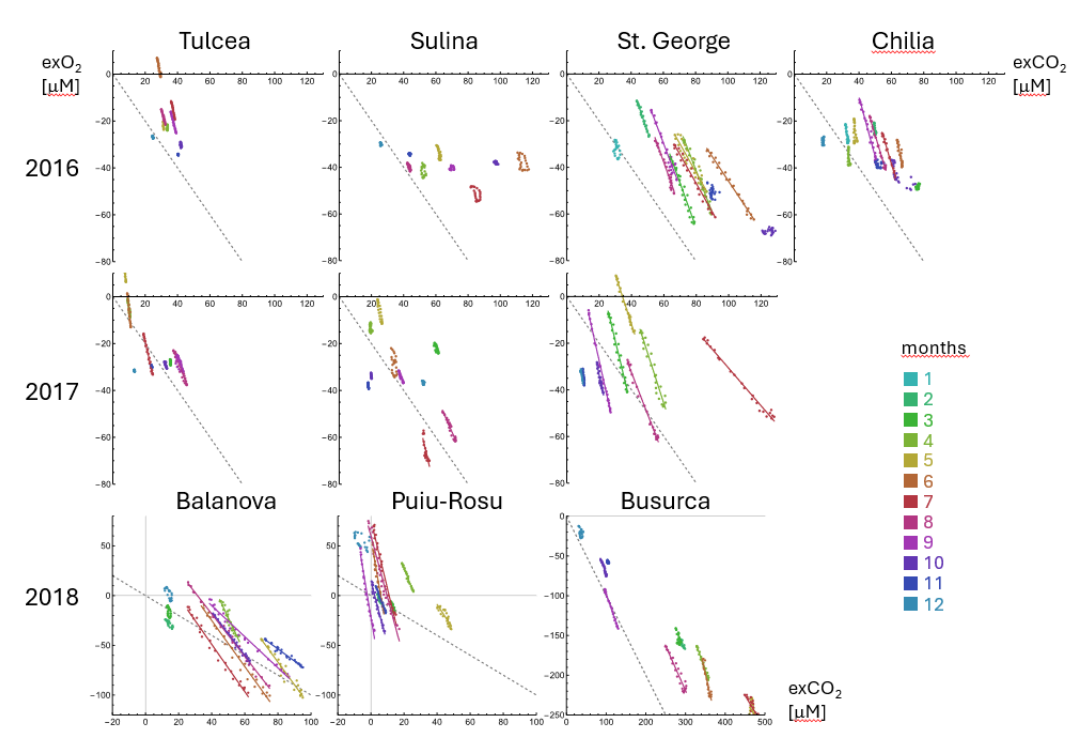


Figure 7. Paired  $exCO_2$  vs  $exO_2$  plots of monthly 24-hour cycles. Dots showing averaged measurements at one hour resolution and their regression lines are color-coded for each month. Grey dotted lines mark theoretical  $CO_2$ - $O_2$  stoichiometry. Same scales for the Danube stations and between Balanova and Puiu-Rosu.





To explore the effect of potential drivers for metabolic intensity at short timescales, we correlated stretch factors [μM] of the daily ex-CO<sub>2</sub>-exO<sub>2</sub> cycles with daily averaged water temperature recordings from the EXO2 probes and the cloud-cover observations from Tulcea airport (Table 4). As expected, there was a negative correlation between average daily cloud cover blocking sunlight and the diel stretch parameters for the ten analysed annual time series. The Pearson's coefficients ρ ranged between -0.11 at Sulina in 2016 and -0.43 at Puiu-Rosu. The rather weak correlation was not surprising given the distance of > 150 km between Tulcea airport and the sampling stations. In addition, the relation between cloud cover, photosynthetically active radiation (Kathilankal et al., 2014) and metabolic response is rather complex in multiyear (Dodds et al., 2013) or multisite analyses (Mulholland et al., 2001). As cloud cover spans the range of 0 to 100%, the cloud-sensitivity of the stretch factor may explain between 7 and 58 μM of stretch variability at Tulcea and Puiu-Rosu, respectively. On average, the cloud-cover sensitivity of the stretch factor was ~4 times larger at the delta stations compared to the river sections.

As expected, water temperature has been identified as a dominant variable for respiration rates in streams (Perkins et al., 2012). In this study, the correlation between average daily water temperatures and the stretch parameters as a measure of metabolic intensity was rather strong (range  $0.37 < \rho < 0.77$ ) for the ten annual records (Table 4). On average, increasing water temperature accelerated metabolic activity at the river stations by  $0.7 \,\mu\text{M}/^{\circ}\text{C}$  and within the delta by  $2.8 \,\mu\text{M}/^{\circ}\text{C}$ . For a seasonal shift in water temperature of  $20^{\circ}\text{C}$  the corresponding change in the stretch parameter amounted to 14 and  $56 \,\mu\text{M}$  for typical Danube River reaches and delta channels, respectively. This fourfold difference in the temperature-sensitivity of the daily stretch parameter between river and delta mirrors the metabolic reaction to cloud cover. We may therefore infer that the daily metabolic activity within the delta network was about a factor four more intense than in the main river reaches.

**Table 4.** Pearson's correlation coefficient  $\rho$  of daily stretch values and daily averages of cloud cover at Tulcea Airport and average local water temperature. Bold face for  $|\rho| > 0.5$  and grey font for  $|\rho| < 0.2$ 

time series		stretch [μM] v	s. cloud cover [%]	stretch [μM] vs. water temp. [°C				
station	year	ρ	slope [µM/ %]	ρ	slope [µM /°C]			
Tulcea	2016	-0.36	-0.07	0.53	0.40			
	2017	-0.40	-0.10	0.70	0.79			
Sulina	2016	-0.11	-0.02	0.41	slope [μM /°C 0.40			
	2017	-0.30	-0.07	0.38	0.36			
St. George	2016	-0.27	-0.13	0.42	0.64			
	2017	-0.27	-0.28	0.41	1.83			
Chilia	2016	-0.29	-0.12	0.48	0.65			
Balanova	2018	-0.34	-0.47	0.77	3.84			
Puiu-Rosu	2018	-0.43	-0.58	0.69	3.25			
Busurca	2018	-0.21	-0.20	0.37	1.44			

465





#### 4.4 Pathways of carbon turnover

As outlined by Vachon et al. (2020), additional processes like carbonate precipitation will affect the position and slope of covariance ellipses. Based on previous regional (Maier et al., 2022) and temporal surveys (Canning et al., 2021) in the Danube Delta, we can expect significant contributions of CH<sub>4</sub> oxidation to O<sub>2</sub>-CO<sub>2</sub> dynamics. Methanotrophic bacteria (Oswald et al., 2016) effectively compete for O<sub>2</sub> (Mayr et al., 2020) with microbial communities involved in the oxic respiration of organic matter (Eq. 1) in a chemoautotrophic process to oxidize CH<sub>4</sub> with O<sub>2</sub> (Eq. 2).

"CH<sub>2</sub>O" + O<sub>2</sub> 
$$\leftrightarrow$$
 CO<sub>2</sub> + H<sub>2</sub>O heterotrophic respiration (1)

475 
$$CH_4 + 2O_2 \leftrightarrow CO_2 + 2 H_2O$$
 methane oxidation (2)

In case of intense methane oxidation, the 24-hour plots in Fig. 7 will approach a slope of -2 or an ecosystem quotient of -1/2. Other oxidative pathways of reduced substances like nitrification, consume oxygen and CO<sub>2</sub> which further steepens the slope of exO<sub>2</sub> vs. exCO<sub>2</sub>. During the summer season this is indeed the case at Balanova station and less frequently at Busurca where conditions turned anoxic in May and July (Fig. 5). In both locations high methane concentrations were observed in previous surveys (Maier et al., 2022) and created conditions for intense oxygen consumption with only 50% CO<sub>2</sub> production.

Under conditions of intense photosynthesis, dissolved CO<sub>2</sub> will be depleted to low levels (Eq. 3), so that uptake of HCO<sub>3</sub><sup>-</sup> will become a dominant pathway of photosynthesis, triggering calcite precipitation (Eq. 4) (Many et al., 2024):

485 
$$CO_2 + H_2O \leftrightarrow \text{``CH}_2O\text{''} + O_2$$
 photosynthesis (3)

$$2 \text{ HCO}_3^- + \text{Ca}^{2+} \leftrightarrow \text{``CH}_2\text{O''} + \text{CaCO}_3 + \text{O}_2$$
 with calcite precipitation (4)

The slope of average daily  $exCO_2$ - $exO_2$  patterns turn steeper, as the importance of pathway 4 increases because  $O_2$  is liberated without change in dissolved  $CO_2$ . There was considerable variability in the slopes from covariance and 24-h analysis (Table D1). Due to the larger amplitude of the day-night  $CO_2$ - $O_2$  cycles, the monthly slopes are better constrained in the summer months (April – Sept). Averaging the summer slopes of both the covariance and 24-hour analysis, yields 20 values; 8 of these calculated slopes were steeper than -2.0, 8 were in the range of -1.0 – 2 and 2 had an absolute value < 1. This synopsis provides strong evidence for methane oxidation, nitrification and other processes with high  $O_2$ -demand and limited  $CO_2$ -yield.

The lake system of Puiu-Rosu was an extreme case with summer slopes in the range of -6 to -10 and partial supersaturation with O<sub>2</sub> indicating uptake of HCO<sub>3</sub><sup>-</sup> during calcite precipitation. (Fig 7, Table D1). Additional evidence comes from the time series of conductivity measurements of the Balanova and Puiu-Rosu stations (Fig. 8). In June and July 2018, the conductivity sensor at the Puiu-Rosu lakes recorded a drop from 420 to less than 250 µS cm<sup>-1</sup> and pH reached day-time values of up to 9. The Balanova probe detected a weaker decline after a typical travel time of about 20 days and remained in a pH range below 8 indicating that low-conductivity lake water was mixed with water from the reed stands with higher dissolved CO<sub>2</sub> concentrations. Together these observations show that intense photosynthesis drove dissolved CO<sub>2</sub> to low levels in Lakes Puiu and Rosu. This favoured photosynthetic carbon uptake via HCO<sub>3</sub><sup>-</sup> and triggered calcite precipitation and the drop in conductivity. The example confirms that freshwater carbonate buffering and calcite precipitation can play significant roles in carbon turnover in such shallow systems (Shangguan et al., 2025).

505





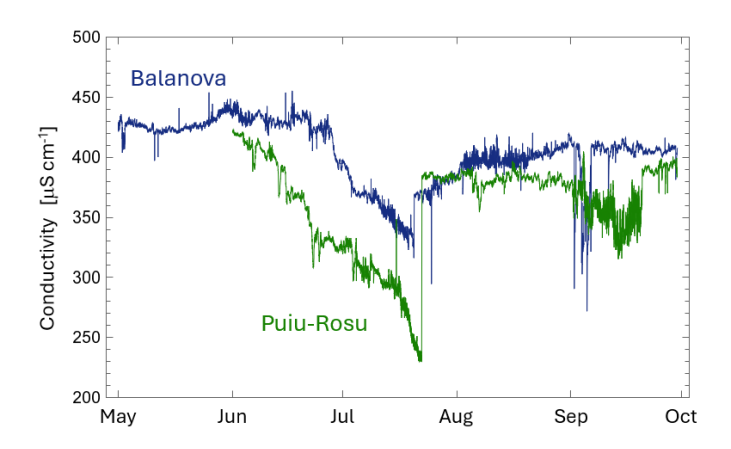


Figure 8. Specific conductivity measured at 15' intervals at Balanova and Puiu-Rosu stations in 2018. The strong reduction in conductivity in the summer months indicates calcite precipitation.

## 5. Conclusion

520

525

This study combined covariance analysis with averaging 24-h cycles of O<sub>2</sub>-CO<sub>2</sub> pairs from sensor measurements at seven locations in the Danube Delta region. The dataset covered 105 monthly and about 3000 daily cycles. Analysing the intensity of O<sub>2</sub>-CO<sub>2</sub> dynamics revealed two orders of magnitude difference in the amplitude of average diel cycles among stations and seasons and a significantly more intense river metabolism within the delta compared to the three main river reaches of the Danube. At monthly timescales, the stations within the delta showed 2-2.5 times higher daily amplitudes in exO<sub>2</sub>-exCO<sub>2</sub> shifts. A daily analysis of potential drivers for river metabolism revealed a factor four stronger sensitivities towards cloud cover and water temperature within the delta compared to the river sections.

The analysis of the shifting averages of excess  $O_2$ - $CO_2$  during an annual cycle allowed us to assess the importance and timing of lateral inflow of  $O_2$ -depleted and  $CO_2$  oversaturated water from adjacent wetlands at monthly timescales. One of the channels drained anoxic wetland water with ex $CO_2$  concentrations of almost 470  $\mu$ M. At downstream Danube stations, strongest inflows from the wetlands were observed in connection to flood peaks in May - June and using an endmember model, these stations recorded mixtures of Danube water enriched by 5-20% wetland water. Attempts failed, however, to predict lateral inflows from upstream water levels due to unknown and variable flow paths and the complex hydrology of flood pulses and flood recession.

Slopes of  $O_2$ -CO<sub>2</sub> covariance ellipses and 24-hour cycles were in many cases significantly steeper than the slope of -1 predicted for a daily cycle of photosynthesis and respiration. Average monthly values for the warm season of April – September revealed ecosystem quotients EQ < 0.5 in 40% of the cases and another 40% were in the range of 0.5 < EQ < 1. Together with the dominant oxygen undersaturation of the lower Danube and its delta system, this was a strong indication for the importance of additional processes with large  $O_2$  demand and low  $CO_2$  yield like methane oxidation and nitrification. In a monitored lake system, a calcite precipitation event was independently recorded by the conductivity sensor in June-July and lead to very low ecosystem quotients  $EQ \sim 0.1$  typical for  $HCO_3$  uptake during photosynthesis.





On a methodological level, the combination of covariance analysis with monthly averages of 24-h cycles provided a complementary perspective for a system, where lateral inflows obscure the in-stream metabolism at monthly timescales. The 24-h analysis provided additional insights into the timing and amplitude of the daily O<sub>2</sub>-CO<sub>2</sub> cycles, whereas covariance analysis was a robust and rapid tool for exploring lateral inflows at monthly timescales and for quantifying metabolic drivers such as temperature and cloud cover at daily resolution.

## 6. Appendices

## 6.1 Appendix A - Monitoring stations

The monitoring stations were located upstream of the Delta at Tulcea and downstream in the three branches of the Danube at St. George, Sulina and Chilia (Fig 1). During the last year, the sensors were relocated to Balanova, Busurca Channel and Puiu-Rosu within the Delta. Time coverage during the field campaign was between 11 and 20 months (Table A1). Spike removal at Sulina and Busurca reduced the number of observation days (Section 2.2.). Due to logistical reasons the mooring of the sensors was usually from anchored boats (Fig. A1).

550 Table A1 Time series of O2-CO2 observations

Station	start data	end date	Full years	N months *	N full days **
Tulcea	31.10.2015	07.02.2018	2016, 2017	20	649
St. George	29.10.2015	09.02.2018	2016, 2017	21	665
Sulina	28.10.2015	30.01.2018	2016, 2017	19	465
Chilia	30.10.2015	13.01.2017	2016	12	357
Balanova	09.02.2018	13.12.2018	2018	11	303
Busurca	10.02.2018	11.12.2018	2018	11	246
Puiu-Rosu	12.02.2018	12.12.2018	2018	11	302
Total				105	2987

<sup>\*</sup>months with >500 data, \*\* days with > 85 data









580

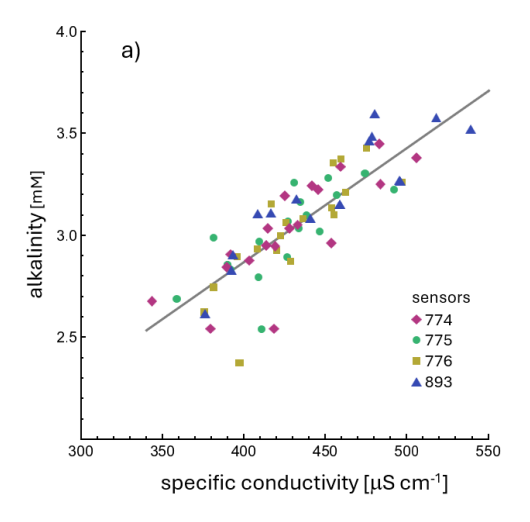


Figure A1 Characteristics of monitoring sites.

a) The Chilia site was located on the Romanian side of a small branch that defines the border with Ukraine. Despite the location in a side-arm, the water had the same chemical signature as the main branch at the time of installation. b) EXO2 probe at Chilia site during winter conditions. c) Clear waters from Busurca channel entering the Sulina reach of the Danube from the right. The Busurca monitoring station was located 25 m upstream of the junction with the Sulina branch. d) Sulina sensor located about 1 km downstream of Busurca junction. The Sulina probe was initially installed in the jetties but due to sporadic increases in specific conductivity, the probe was moved 3 km upstream in February 2016 to avoid disturbance by Black Sea water. It was moored at an old, 565 anchored ship. e) View from Tartaru channel which was monitored at Balanova station towards the St. George Branch with the turbid Danube waters flowing from left to right. f) For logistical reasons, the monitoring at St. George branch was located about 500 m downstream of Tartaru junction. The Black Sea is visible on the horizon. g) The Busurca probe was moored on a small, anchored houseboat. h) The Puiu-Rosu sensor recorded water quality at the outlet of Lake Puiu. The station was located on a small channel connecting Lake Puiu with Lake 570 Rosu. i) The Balanova multiprobe was placed in the Central Channel that connects Sulina and St. George main branches and runs in parallel to the gravel road connecting the two communities. The location is characterized by water from Lake Rosu that enters the Central Channel via the Andrei channel and splits north and south towards Sulina and St. George, respectively. At this location, water generally returns to the Danube after its journey through the intricate network of channels and lakes within the Delta. Not shown: The Tulcea station, where sensors monitored Danube water at the apex of the delta. The station was located 300 m downstream of the bifurcation of the Tulcea and Chilia branch.

## 6.2 Appendix B - Calculation of CO2

The EXO2 sensors measured pH, temperature and specific conductivity at a frequency of 15 minutes. Using grab samples we correlated the continuous conductivity data with discrete lab-based alkalinity measurements and used the COSYS code (Van Heuven et al., 2011) to calculate dissolved CO<sub>2</sub> (Section 2.2).



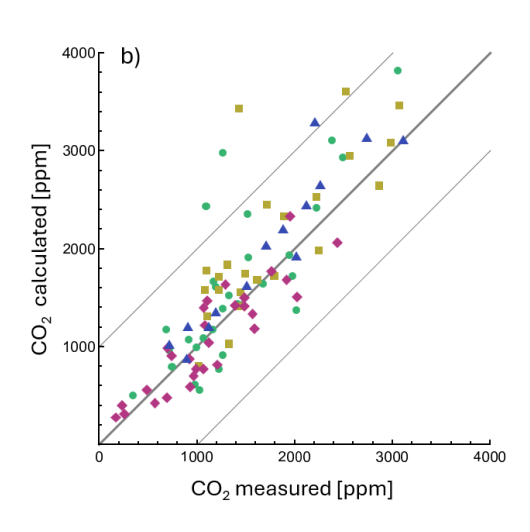




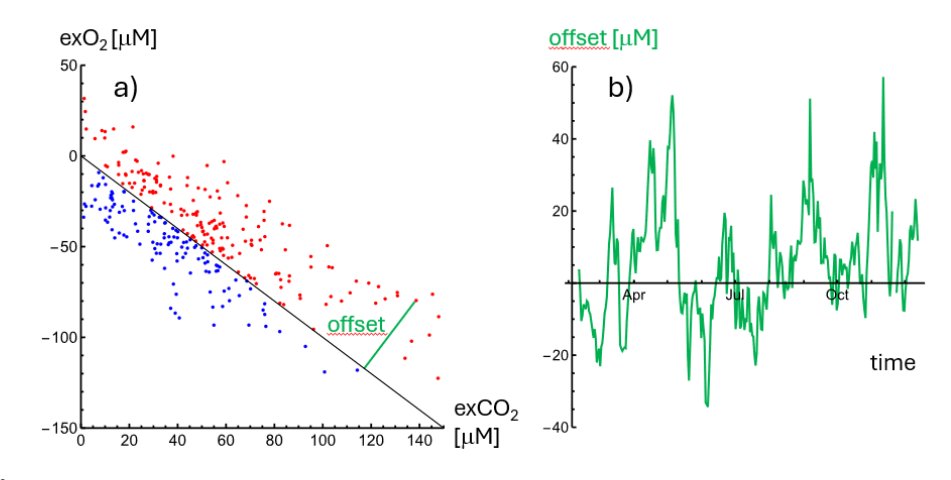


Figure B1 a) Linear regression of alkalinity analyses for water samples and specific conductivity. Labels mark the four different EXO-2 probes deployed. Alkalinity  $[mM] = 0.0057 \times \text{specific conductivity} [\mu S \text{ cm}^{-1}] + 0.60$ , with a correlation coefficient of  $R^2 = 0.70$ . The specific conductivity recorded by the EXO2 sensors was correlated with alkalinity measurements obtained from titration analysis of water samples taken the same time and location. The coloured symbols mark the sensor codes, because the location of sensor packages changed during the three years of observations.

b). Measured CO2 data based on the headspace technique compared to dissolved CO2 calculated from EXO2 data (specific conductivity, pH and temperature. Alkalinity estimated from the correlation shown in panel a) and pH plus temperature records were combined to calculate dissolved CO2. These CO2 estimates compared well with direct CO2 measurements. With few exceptions, the points lie well within the 1:1 relationship ± 1000 ppm. Symbols represent sensors as in panel a).

## 595 6.3 Appendix C: Offset and slope

The offset can be defined with a positive or negative sign depending on the centroid position. Here we illustrate the definition and the construction of well-resolved offset timeseries (Fig. C1).



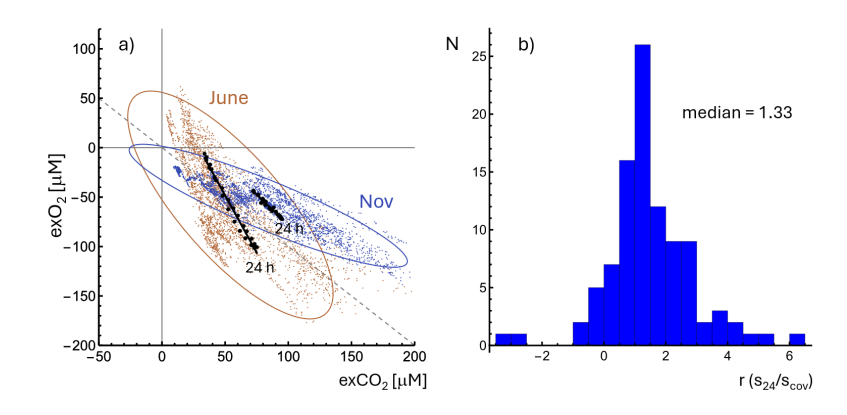
600

Figure C1 a) Daily centroids (average  $\mu$ M concentrations) of exCO<sub>2</sub> and exO<sub>2</sub> pairs at Balanova station in 2018. The closest distance between the dots and the line with slope -1 defines the offset. The green line shows an example. Blue dots are characterized by a negative offset and occur when high rates of photosynthesis and respiration reduce both O<sub>2</sub> and CO<sub>2</sub>. We calculated the  $\Sigma = \exp CO_2 + \exp O_2$  and defined a positive offset for  $\Sigma > 0$ , and negative offsets for  $\Sigma < 0$ . b) Time series of the resulting offset [ $\mu$ M] at Balanova station in 2018 shows phases where respiration dominates with a surplus in  $\exp CO_2$  (positive offset) and periods in spring and summer when photosynthesis depleted the  $\exp CO_2$  pool in comparison to  $\exp O_2$ . This time series with daily offsets is compatible with the trajectories of the monthly centroids (Fig. 5).





The slopes of the stretch axes of the covariance ellipses (Fig 2) are defined by the Eigenvectors of the covariance matrix. By contrast, the slope of monthly averaged 24-hour cycles can be obtained from regression analysis. The slopes are related to the process stoichiometry of the river metabolism via the Ecosystem Quotient EQ = 1/s. Here we compare the two calculation methods.



620

Figure C2 a) Examples of monthly covariance ellipses for June and November 2018 at Balanova. Black dots are the 24-hour monthly averages of daily fluctuations. The black regression lines show steeper slopes compared to the tilt of the covariance ellipses. b) Histogram of slope ratios  $r = s_{24}/s_{cov}$  where  $s_{24}$  stands for the slope of the monthly averaged 24-hour cycle and  $s_{cov}$  refers to the tilt of the covariance ellipse calculated from the Eigenvectors of the covariance matrix. A total of 105 monthly records were analysed (Table D1). The median of r was 1.33 indicating that covariance analysis underestimates the slope of the day-night cycles. In the Danube Delta lateral inflow of CO<sub>2</sub>-rich water shifts the daily O<sub>2</sub>-CO<sub>2</sub> cycles on the horizontal axis which decreases the observed average monthly slope. To avoid this artifact, slopes and corresponding ecosystem quotients EQ should preferably be calculated from averaged 24-hour cycles.





## 6.4 Appendix D: Results from 24-h averaging and covariance analysis

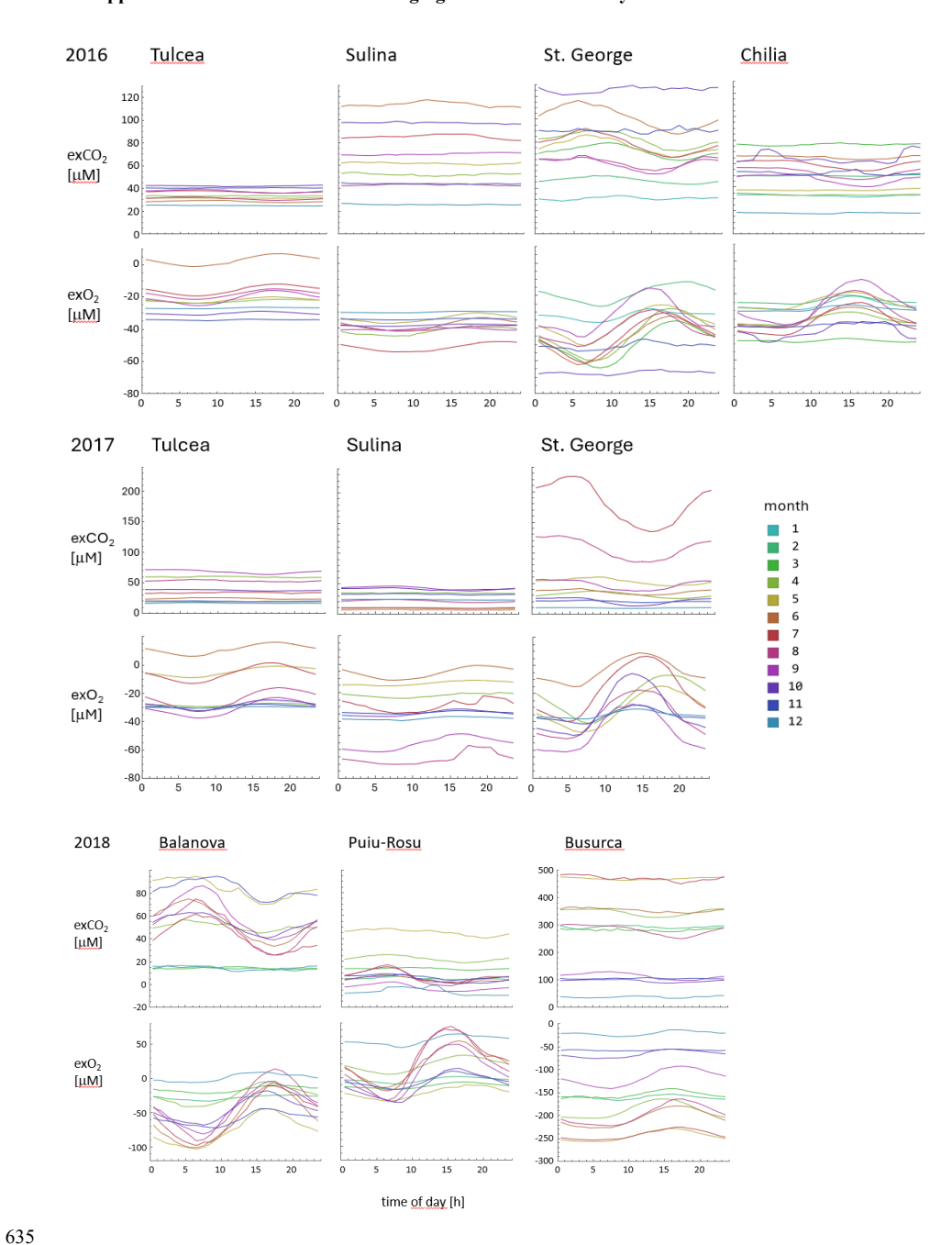


Figure D1. Monthly averaged time-of-day plots at 15-minute resolution showing excess CO<sub>2</sub> and O<sub>2</sub> for the years 2016 and 2017 at the Danube stations of Tulcea, Sulina, St. George, and Chilia and for the three stations within the Delta in 2018. Note that the months are color coded and y-axes in 2016 and 2017 differ. In comparison to Balanova and Puiu-Rosu, data from the Busurca Channel are plotted with an extended y-axis.





Table D1 Results of monthly covariance analysis. Centroid position c-exCO<sub>2</sub> and c-exO<sub>2</sub>, stretch, width and offset  $[\mu M]$ , slope [-]. Maximum number of observations (ndata) for 31 days is 2976., slope-24 refers to the slope calculated from 24-h averaging (Fig 7, Fig S4f)), nd = no data.

Station	parameter	Jan	Feb	Mar	Apr	May	Jun	Jul	Aug	Sept	Oct	Nov	Dec
Tulcea	ndata	1793	nd	nd	1879	2468	1967	2971	2971	2875	2970	2874	2770
2016	c-exCO <sub>2</sub>	35.9	nd	nd	33.8	31.3	28.5	37.2	31.2	37.4	42.1	40.4	24.7
	c-exO <sub>2</sub>	-26.8	nd	nd	-22.7	-21.8	2.8	-15.5	-18.2	-20.6	-30.3	-34.3	-26.9
	stretch	11.8	nd	nd	19.7	42.2	54.5	46.3	40.1	30.9	38.8	13.0	16.4
	width	5.4	nd	nd	4.5	11.3	16.7	20.6	10.3	10.6	6.6	4.9	4.6
	offset	6.4	nd	nd	7.8	6.7	22.2	15.4	9.2	11.9	8.3	4.3	1.5
	slope	0.6	nd	nd	-1.3	-1.4	-1.7	-1.9	-3.6	-1.8	-1.7	-0.7	-0.6
	slope-24	nd	nd	nd	-3.6	-3.7	-3.4	-3.5	-2.6	-2.7	-1.2	+0.3	-1.3
Tulcea	ndata	nd	nd	2976	2873	2969	2873	2969	2969	2872	2619	2875	1822
2017	c-exCO <sub>2</sub>	nd	nd	35.6	9.9	7.5	10.1	21.6	41.9	41.1	32.7	23.9	13.3
	c-exO <sub>2</sub>	nd	nd	-27.9	-4.8	11.3	-5.9	-24.2	-30.6	-28.2	-29.2	-29.7	-31.5
	stretch	nd	nd	29.7	51.2	78.0	61.1	64.4	54.3	35.6	20.1	14.0	7.7
	width	nd	nd	7.5	17.7	6.3	12.1	15.1	11.0	11.2	9.2	6.5	5.3
	offset	nd	nd	5.4	3.7	13.3	2.9	1.8	8.0	9.1	2.4	4.1	12.9
	slope	nd	nd	-4.3	-1.9	-3.1	-6.0	-1.9	-1.5	-0.9	-1.9	0.4	-1.5
	slope-24	nd	nd	-2.4	-4.5	-8.2	-6.5	-3.1	-1.8	-1.3	-1.7	-1.3	-0.6
St George	ndata	2971	2779	2971	2875	2971	2876	2972	2971	1872	1774	1486	nd
2016	c-exCO <sub>2</sub>	31.0	47.2	71.8	81.9	76.3	101.6	78.7	61.9	61.7	125.8	90.2	nd
	c-exO <sub>2</sub>	-32.3	-18.7	-49.5	-44.3	-37.3	-47.2	-44.8	-41.1	-32.6	-67.3	-50.7	nd
	stretch	28.0	42.6	50.4	63.7	53.2	59.8	45.7	38.9	37.8	73.5	48.9	nd
	width	18.1	9.9	20.3	20.5	18.0	14.7	17.0	17.6	12.4	13.9	22.8	nd
	offset	0.9	20.2	15.8	26.6	27.6	38.5	23.9	14.7	20.5	41.3	27.9	nd
	slope	-1.3	-1.6	-1.0	-1.0	-0.9	-0.8	-0.9	-1.1	-1.4	-0.4	-0.4	nd
	slope-24	-0.7	-2.0	-1.9	-1.8	-1.2	-1.0	-1.2	-1.9	-1.8	+0.1	-0.5	nd
St George	ndata	nd	nd	2818	2873	2967	2149	2970	2963	2184	1299	2874	2770
2017	c-exCO <sub>2</sub>	nd	nd	31.3	53.2	36.1	180.7	106.8	48.0	21.5	20.6	10.4	9.3
	$c$ - $exO_2$	nd	nd	-22.9	-31.2	-3.7	-17.0	-36.2	-46.9	-32.2	-35.5	-35.0	-33.5
	stretch	nd	nd	44.9	68.8	62.1	225.0	151.3	76.0	50.2	16.4	13.1	16.8
	width	nd	nd	16.1	27.8	16.6	38.4	55.8	27.9	15.1	12.9	7.6	12.2
	offset	nd	nd	6.0	15.5	22.9	115.7	49.9	0.7	7.6	10.5	17.4	17.1
	slope	nd	nd	-2.3	-0.9	-1.7	-0.2	0.0	-0.7	-2.2	-3.5	-6.4	-0.6
	slope-24	nd	nd	-2.9	-2.1	-2.1	-0.5	-0.8	-1.8	-3.1	-3.2	-5.6	-3.1
Sulina	ndata	nd	nd	nd	792	2692	1593	2969	2967	2487	2969	2872	2966
2016	c-exCO <sub>2</sub>	nd	nd	nd	52.3	62.0	113.7	85.2	43.3	69.9	97.3	43.8	25.8
	$c$ - $exO_2$	nd	nd	nd	-41.5	-34.0	-37.9	-51.7	-39.8	-40.3	-38.0	-34.4	-30.1
	stretch	nd	nd	nd	18.9	50.3	58.4	52.8	24.7	44.4	59.9	21.2	18.4
	width	nd	nd	nd	7.8	13.6	16.8	21.1	14.3	12.2	16.3	8.1	5.1
	offset	nd	nd	nd	7.7	19.8	53.6	23.7	2.5	20.9	41.9	6.7	3.0
	slope	nd	nd	nd	-1.3	-0.5	-0.5	0.0	-4.9	-0.6	-0.3	-0.3	-0.9
	slope-24	nd	nd	nd	-0.2	-2.2	-0.6	-0.7	-1.3	+0.1	-0.4	-0.3	-0.6





Table D2 - continued

Station	parameter	Jan	Feb	Mar	Apr	May	Jun	Jul	Aug	Sept	Oct	Nov	Dec
Sulina	ndata	nd	nd	1380	1761	2971	1046	1424	1366	1985	2758	510	1382
2017	c-exCO <sub>2</sub>	nd	nd	60.3	19.5	25.1	34.1	53.8	68.8	38.5	19.9	18.1	52.3
	c-exO <sub>2</sub>	nd	nd	-21.9	-13.3	-6.3	-29.3	-66.1	-55.8	-34.5	-33.8	-38.0	-36.7
	stretch	nd	nd	24.6	33.7	71.6	49.1	100.6	40.1	31.1	12.7	9.3	15.7
	width	nd	nd	14.5	19.5	13.3	19.7	40.2	17.7	11.2	6.7	1.2	4.8
	offset	nd	nd	27.2	4.4	13.3	3.4	8.6	9.2	2.8	9.8	14.1	11.0
	slope	nd	nd	-2.1	-1.4	-1.6	-2.4	-3.0	-1.2	-0.8	11.0	-3.3	-0.4
	slope-24	nd	nd	-2.4	-4.5	-8.2	-6.5	-3.1	-1.8	-1.2	-1.7	-1.3	-0.6
Chilia	ndata	2616	2247	2970	2874	2486	2873	2969	2964	2716	1620	2611	2894
2016	c-exCO <sub>2</sub>	32.7	49.8	76.3	33.7	37.4	65.5	59.2	52.3	46.4	64.5	52.1	17.9
	c-exO <sub>2</sub>	-26.6	-24.0	-48.1	-35.7	-25.2	-34.7	-36.5	-31.4	-26.2	-42.3	-38.8	-29.0
	stretch	17.6	21.3	29.5	29.2	48.0	39.4	37.7	42.8	79.2	65.1	29.7	24.3
	width	9.7	7.3	23.7	11.9	11.1	13.9	17.3	17.6	12.5	12.6	10.9	6.5
	offset	4.4	18.2	19.9	1.4	8.6	21.8	16.1	14.8	14.3	15.7	9.4	7.9
	slope	4.8	-0.5	-1.0	-0.9	-0.8	-0.8	-0.8	-1.8	-1.6	-0.6	-0.4	-0.8
	slope-24	-3.8	-2.2	+0.4	-3.0	-2.3	-3.2	-2.3	-2.3	-2.5	-0.7	-0.1	+0.5
Balanova	ndata	nd	1859	2976	2874	2969	2875	2971	2971	2875	2971	2776	1211
2018	c-exCO <sub>2</sub>	nd	14.2	14.0	50.5	83.7	54.2	42.5	49.4	60.1	53.3	84.2	14.2
	c-exO <sub>2</sub>	nd	-28.1	-16.4	-24.3	-75.4	-58.0	-54.9	-38.5	-41.5	-45.4	-58.8	1.2
	stretch	nd	27.6	46.4	74.5	113.4	133.9	124.5	133.1	119.1	59.3	124.2	53.7
	width	nd	15.7	21.2	29.7	54.4	44.3	28.8	36.2	38.7	23.0	23.7	13.7
	offset	nd	9.8	1.7	18.6	5.9	2.7	8.8	7.7	13.1	5.6	18.0	10.9
	slope	nd	-1.7	-31.4	-0.9	-0.6	-1.6	-1.6	-1.3	-1.0	-1.7	-0.5	-1.9
	slope-24	nd	-1.8	-2.9	-3.5	-2.3	-2.3	-2.4	-2.1	-1.6	-2.2	-1.2	-2.9
Busurca	ndata	nd	1767	1513	2455	2860	2452	1011	2417	2868	2972	2874	1020
2018	c-exCO <sub>2</sub>	nd	291	282	346	468	354	469	280	113	94.7	104	36.3
	c-exO <sub>2</sub>	nd	-161	-154	-188	-245	-206	-241	-197	-117	-65.8	-57.7	-20.3
	stretch	nd	111.8	65.4	167.9	90.8	165.0	68.5	265.9	137.3	93.2	146.3	53.2
	width	nd	19.2	32.9	26.5	35.8	45.2	45.6	56.0	40.9	46.9	41.2	27.8
	offset	nd	92.3	90.6	111.4	157.5	104.6	161.3	58.8	2.4	20.4	33.0	11.3
	slope	nd	-0.3	-0.2	-0.6	-0.2	-0.3	0.1	-0.4	-1.2	-0.9	-0.4	-2.6
	slope-24	nd	-0-7	-1.2	-1.4	-0.6	-2.2	-0.8	-1.1	-1.5	-1.4	-0.3	-0.6
PuiuRosu	ndata	nd	1575	2976	2875	2969	2875	2969	2971	2875	2971	2874	1110
2018	c-exCO <sub>2</sub>	nd	5.0	13.2	22.2	45.1	3.9	7.2	6.5	-2.8	4.0	6.2	-6.3
	c-exO <sub>2</sub>	nd	-3.0	-12.1	18.4	-21.9	19.3	26.4	19.6	6.7	-10.8	-5.2	54.6
	stretch	nd	20.2	63.0	35.9	75.1	135.4	133.7	127.6	98.4	78.3	69.0	64.9
	width	nd	17.8	31.5	34.6	39.8	17.9	21.2	26.7	8.9	15.8	17.8	31.1
	offset	nd	1.4	0.8	28.7	16.4	16.4	23.7	18.5	2.7	4.8	0.7	34.1
	slope	nd	24.2	-1.2	-0.4	0.1	-7.8	-5.6	-5.3	-10.0	-3.9	-1.8	-5.4
	slope-24	nd	-3.89	-4.2	-4.2	-2.6	-9.7	-6.9	-6.1	-10.0	-6.3	-4.5	-1.2





#### 7. Code availability

The Mathematica code is available as a notebook file at GitHub <a href="https://github.com/bernhardwehrli/CO2-O2-stat">https://github.com/bernhardwehrli/CO2-O2-stat</a>

## 8. Data availability

Timeseries data and the calculated daily covariance parameters for all stations are available at the ETH research collection via <a href="https://doi.org/10.3929/ethz-c-000786936">https://doi.org/10.3929/ethz-c-000786936</a>

#### 9. Author contributions

655 Field campaigns and statistical analyses were designed with input from all authors, BW provided project supervision, CT led the monitoring campaigns and data collection, MSM was responsible for post-processing and quality control of field data and calculated the exCO<sub>2</sub> and exO<sub>2</sub> timeseries. BW led the coding, drafting and writing of the paper with continuous input from MSM and CT.

## 10. Competing interests

The authors declare that they have no conflict of interest.

## 11. Acknowledgements

The authors thank Christian Dinkel, Patrick Kathriner and Tim Kalvelage for their support during fieldwork and lab analyses.

## 12. Financial support

This study was supported by the Swiss State Secretariat for Education, Research and Innovation (SERI; grant no. 15.0068). The research consortium received funding from the European Union's Horizon 2020 research and innovation programme under the Marie- Skłodowska-Curie-Actions (grant no. 643052; C-CASCADES project). The Swiss National Science Foundation (SNF) and Eawag provided funding for the EXO2 probes (R'EQUIP 157750).

## 670 13. References

- Abril, G. and Borges, A. V.: Ideas and perspectives: Carbon leaks from flooded land: do we need to replumb the inland water active pipe?, Biogeosciences, 16, 769-784, 10.5194/bg-16-769-2019, 2019.
- Aho, K. S., Hosen, J. D., Logozzo, L. A., McGillis, W. R., and Raymond, P. A.: Highest rates of gross primary productivity maintained despite CO<sub>2</sub> depletion in a temperate river network, Limnology and Oceanography Letters, 6, 200-206, 10.1002/lol2.10195, 2021.
- Battin, T. J., Lauerwald, R., Bernhardt, E. S., Bertuzzo, E., Gener, L. G., Hall, R. O., Jr., Hotchkiss, E. R., Maavara, T., Pavelsky, T. M., Ran, L., Raymond, P., Rosentreter, J. A., and Regnier, P.: River ecosystem metabolism and carbon biogeochemistry in a changing world, Nature, 613, 449-459, 10.1038/s41586-022-05500-8, 2023.
- 680 Bernhardt, E. S., Heffernan, J. B., Grimm, N. B., Stanley, E. H., Harvey, J. W., Arroita, M., Appling, A. P., Cohen, M. J., McDowell, W. H., Hall, R. O., Read, J. S., Roberts, B. J., Stets, E. G., and Yackulic, C. B.: The metabolic regimes of flowing waters, Limnology and Oceanography, 63, 10.1002/lno.10726, 2017.





- Bondar, C.: Referitor la alimentarea si tranzitul apelor Dunarii prin interiorul deltei, Analele ICPDD, III/2, 259-261, 1994.
- 685 Borges, A. V., Darchambeau, F., Lambert, T., Morana, C., Allen, G. H., Tambwe, E., Sembaito, A. T., Mambo, T., Wabakhangazi, J. N., Descy, J. P., Teodoru, C. R., and Bouillon, S.: Variations in dissolved greenhouse gases (CO<sub>2</sub>, CH<sub>4</sub>, N<sub>2</sub>O) in the Congo River network overwhelmingly driven by fluvial-wetland connectivity, Biogeosciences, 16, 3801-3834, 10.5194/bg-16-3801-2019, 2019.
- Cai, W. J. and Wang, Y.: The chemistry, fluxes, and sources of carbon dioxide in the estuarine waters of the Satilla and Altamaha Rivers, Georgia, Limnology and Oceanography, 43, 657-668, 1998.
  - Canning, A., Wehrli, B., and Körtzinger, A.: Methane in the Danube Delta: the importance of spatial patterns and diel cycles for atmospheric emission estimates, Biogeosciences, 18, 3961-3979, 10.5194/bg-18-3961-2021, 2021.
- Cole, J. J., Prairie, Y. T., Caraco, N. F., McDowell, W. H., Tranvik, L. J., Striegl, R. G., Duarte, C. M., Kortelainen,
  P., Downing, J. A., Middelburg, J. J., and Melack, J.: Plumbing the Global Carbon Cycle: Integrating Inland
  Waters into the Terrestrial Carbon Budget, Ecosystems, 10, 172-185, 10.1007/s10021-006-9013-8, 2007.
  - Dalmagro, H. J., Lathuilliere, M. J., Hawthorne, I., Morais, D. D., Pinto, O. B., Couto, E. G., and Johnson, M. S.: Carbon biogeochemistry of a flooded Pantanal forest over three annual flood cycles, Biogeochemistry, 139, 1-18, 10.1007/s10533-018-0450-1, 2018.
- 700 Degens, E., Kempe, S., and Ittekkot, V.: Monitoring carbon in world rivers, Environment: Science and Policy for Sustainable Development, 26, 29-33, 10.1080/00139157.1984.9932533, 1984.
  - Deirmendjian, L. and Abril, G.: Carbon dioxide degassing at the groundwater-stream-atmosphere interface: isotopic equilibration and hydrological mass balance in a sandy watershed, Journal of Hydrology, 558, 129-143, 10.1016/j.jhydrol.2018.01.003, 2018.
- 705 DelVecchia, A. G., Rhea, S., Aho, K. S., Stanley, E. H., Hotchkiss, E. R., Carter, A., and Bernhardt, E. S.: Variability and drivers of CO<sub>2</sub>, CH<sub>4</sub>, and N<sub>2</sub>O concentrations in streams across the United States, Limnology and Oceanography, 68, 394-408, 10.1002/lno.12281, 2023.
  - Dodds, W. K., Veach, A. M., Ruffing, C. M., Larson, D. M., Fischer, J. L., and Costigan, K. H.: Abiotic controls and temporal variability of river metabolism: multiyear analyses of Mississippi and Chattahoochee River data, Freshwater Science, 32, 1073-1087, 10.1899/13-018.1, 2013.
  - Gatescu, P., Driga, B., and Angel, C.: Caracteristici morfohidrografice ale Deltei Dunarii, Hidrobiologia, Acad. Rom. Bucuresti 1983.
- Gomez-Gener, L., Rocher-Ros, G., Battin, T., Cohen, M. J., Dalmagro, H. J., Dinsmore, K. J., Drake, T. W., Duvert, C., Enrich-Prast, A., Horgby, A., Johnson, M. S., Kirk, L., Machado-Silva, F., Marzolf, N. S., McDowell, M. J., McDowell, W. H., Miettinen, H., Ojala, A. K., Peter, H., Pumpanen, J., Ran, L. S., Riveros-Iregui, D. A., Santos, I. R., Six, J., Stanley, E. H., Wallin, M. B., White, S. A., and Sponseller, R. A.: Global carbon dioxide efflux from rivers enhanced by high nocturnal emissions, Nature Geoscience, 14, 289-+, 10.1038/s41561-021-00722-3, 2021.
- Haque, M. M., Begum, M. S., Nayna, O. K., Tareq, S. M., and Park, J.-H.: Seasonal shifts in diurnal variations of CO<sub>2</sub> and O<sub>2</sub> in the lower Ganges River, Limnology and Oceanography Letters, 7, 191-201, 10.1002/lol2.10246, 2022.
  - Hotchkiss, E. R., Hall Jr, R. O., Sponseller, R. A., Butman, D., Klaminder, J., Laudon, H., Rosvall, M., and Karlsson, J.: Sources of and processes controlling CO<sub>2</sub> emissions change with the size of streams and rivers, Nature Geoscience, 8, 696-699, 10.1038/ngeo2507, 2015.
- 725 Huertas, I. E., Flecha, S., Figuerola, J., Costas, E., and Morris, E. P.: Effect of hydroperiod on CO<sub>2</sub> fluxes at the air-water interface in the Mediterranean coastal wetlands of Donana, Journal of Geophysical Research-Biogeosciences, 122, 1615-1631, 10.1002/2017JG003793, 2017.
  - ICPDR: On the implementation of the joint program of measures in the Danube River basin 2018, 2018.
- Kathilankal, J. C., O'Halloran, T. L., Schmidt, A., Hanson, C. V., and Law, B. E.: Development of a semiparametric PAR (Photosynthetically Active Radiation) partitioning model for the United States, version 1.0, Geoscientific Model Development, 7, 2477-2484, 10.5194/gmd-7-2477-2014, 2014.
  - Maier, M.-S., Teodoru, C. R., and Wehrli, B.: Spatio-temporal variations in lateral and atmospheric carbon fluxes from the Danube Delta, Biogeosciences, 18, 1417-1437, 10.5194/bg-18-1417-2021, 2021.
- Maier, M.-S., Canning, A. R., Brennwald, M. S., Teodoru, C. R., and Wehrli, B.: Spatial Mapping of Dissolved
  Gases in the Danube Delta Reveals Intense Plant-Mediated Gas Transfer, Frontiers in Environmental
  Science, 10, 10.3389/fenvs.2022.838126, 2022.
  - Many, G., Escoffier, N., Perolo, P., Barenbold, F., Bouffard, D., and Perga, M. E.: Calcite precipitation: The forgotten piece of lakes' carbon cycle, Science Advances, 10, eado5924, 10.1126/sciadv.ado5924, 2024.
- Marzolf, N. S., Small, G. E., Oviedo-Vargas, D., Ganong, C. N., Duff, J. H., Ramirez, A., Pringle, C. M., Genereux,
   D. P., and Ardon, M.: Partitioning inorganic carbon fluxes from paired O<sub>2</sub>-CO<sub>2</sub> gas measurements in a Neotropical headwater stream, Costa Rica, Biogeochemistry, 160, 259-273, 10.1007/s10533-022-00954-4, 2022.





755

765

- Mayr, M. J., Zimmermann, M., Dey, J., Brand, A., Wehrli, B., and Burgmann, H.: Growth and rapid succession of methanotrophs effectively limit methane release during lake overturn, Communications Biology, 3, 108, 10.1038/s42003-020-0838-z, 2020.
- Mulholland, P. J., Fellows, C. S., Tank, J. L., Grimm, N. B., Webster, J. R., Hamilton, S. K., Martí, E., Ashkenas, L., Bowden, W. B., Dodds, W. K., McDowell, W. H., Paul, M. J., and Peterson, B. J.: Inter-biome comparison of factors controlling stream metabolism, Freshwater Biology, 46, 1503-1517, 10.1046/j.1365-2427.2001.00773.x, 2001.
- 750 Oosterberg, W., Staras, M., Bodgdan, L., Buijse, A. D., Constantinescu, A., Coops, H., Hanganu, J., Ibelings, B. W., Menting, G. A. M., and Navodaru, I.: Ecological gradients in the Danube Delta lakes: present state and man-induced changes, RIZA, Rijkswaterstaat, NL, 2000.
  - Oswald, K., Milucka, J., Brand, A., Hach, P., Littmann, S., Wehrli, B., Kuypers, M. M. M., and Schubert, C. J.:
    Aerobic gammaproteobacterial methanotrophs mitigate methane emissions from oxic and anoxic lake waters, Limnology and Oceanography, 61, 10.1002/lno.10312, 2016.
  - Perkins, D. M., Yvon-Durocher, G., Demars, B. O. L., Reiss, J., Pichler, D. E., Friberg, N., Trimmer, M., and Woodward, G.: Consistent temperature dependence of respiration across ecosystems contrasting in thermal history, Global Change Biology, 18, 1300-1311, 10.1111/j.1365-2486.2011.02597.x, 2012.
- Rabaey, J. S., Holgerson, M. A., Richardson, D. C., Andersen, M. R., Bansal, S., Bortolotti, L. E., Cotner, J. B.,
   Hornbach, D. J., Martinsen, K. T., Moody, E. K., and Schloegel, O. F.: Freshwater Biogeochemical Hotspots: High Primary Production and Ecosystem Respiration in Shallow Waterbodies, Geophysical Research Letters, 51, 10.1029/2023g1106689, 2024.
  - Reiman, J. H. and Xu, Y. J.: Dissolved carbon export and CO<sub>2</sub> outgassing from the lower Mississippi River Implications of future river carbon fluxes, Journal of Hydrology, 578, 10.1016/j.jhydrol.2019.124093, 2019.
  - Renaud, F. G., Syvitski, J. P. M., Sebesvari, Z., Werners, S. E., Kremer, H., Kuenzer, C., Ramesh, R., Jeuken, A., and Friedrich, J.: Tipping from the Holocene to the Anthropocene: How threatened are major world deltas?, Current Opinion in Environmental Sustainability, 5, 644-654, 10.1016/j.cosust.2013.11.007, 2013.
- Rocher-Ros, G., Gomez-Gener, L., Jativa, C., Lannergård, E. E., Laudon, H., Lupon, A., Martí, E., Peñarroya, X.,
  Sponseller, R. A., and Bernal, S.: Emerging patterns of CO<sub>2</sub>: O<sub>2</sub> dynamics in rivers and their link to
  ecosystem carbon processing, Limnology and Oceanography Letters, 10.1002/lol2.70057, 2025.
  - Rode, M., Wade, A. J., Cohen, M. J., Hensley, R. T., Bowes, M. J., Kirchner, J. W., Arhonditsis, G. B., Jordan, P., Kronvang, B., Halliday, S. J., Skeffington, R. A., Rozemeijer, J. C., Aubert, A. H., Rinke, K., and Jomaa, S.: Sensors in the Stream: The High-Frequency Wave of the Present, Environmental Science and Technology, 50, 10297-10307, 10.1021/acs.est.6b02155, 2016.
  - Romanova, Y., Shakirzanova, Z., Ovcharuk, V., Todorova, O., Medvedieva, I., and Ivanchenko, A.: Temporal variation of water discharges in the lower course of the Danube River across the area from Reni to Izmail under the influence of natural and anthropogenic factors, Energetika, 65, 144-160, 10.6001/energetika.v65i2-3.4108, 2019.
- 780 Rosentreter, J. A., Laruelle, G. G., Bange, H. W., Bianchi, T. S., Busecke, J. J. M., Cai, W.-J., Eyre, B. D., Forbrich, I., Kwon, E. Y., Maavara, T., Moosdorf, N., Najjar, R. G., Sarma, V. V. S. S., Van Dam, B., and Regnier, P.: Coastal vegetation and estuaries are collectively a greenhouse gas sink, Nature Climate Change, 13, 579-587, 10.1038/s41558-023-01682-9, 2023.
- Sabater, S., Timoner, X., Borrego, C., and Acuña, V.: Stream Biofilm Responses to Flow Intermittency: From Cells to Ecosystems, Frontiers in Environmental Science, 4, 10.3389/fenvs.2016.00014, 2016.
  - Shangguan, Q. P., Degrandpre, M. D., Hall, R. O., Jr., and Payn, R. A.: Freshwater carbonate buffering revisited, Limnology and Oceanography Letters, 10, 619-635, 10.1002/lol2.70047, 2025.
- Solano, V., Duvert, C., Birkel, C., Maher, D. T., Garcia, E. A., and Hutley, L. B.: Stream respiration exceeds CO<sub>2</sub> evasion in a low-energy, oligotrophic tropical stream, Limnology and Oceanography, 68, 1132-1146, 10.1002/lno.12334, 2023.
  - Vachon, D., Sadro, S., Bogard, M. J., Lapierre, J. F., Baulch, H. M., Rusak, J. A., Denfeld, B. A., Laas, A., Klaus, M., Karlsson, J., Weyhenmeyer, G. A., and Giorgio, P. A.: Paired O<sub>2</sub> CO<sub>2</sub> measurements provide emergent insights into aquatic ecosystem function, Limnology and Oceanography Letters, 5, 287-294, 10.1002/lol2.10135, 2020.
- van Heuven, S., Pierrot, D., Rae, J. W. B., Lewis, E., and Wallace, D. W. R.: MATLAB Program Developed for CO<sub>2</sub> System Calculations, Carbon Dioxide Information Analysis Center, Oak Ridge National Laboratory, U.S. Department of Energy, Oak Ridge, Tennessee, 10.3334/CDIAC/otg.CO2SYS MATLAB v1.1, 2011.
  - Weiss, R. F.: Carbon dioxide in water and seawater: the solubility of a non-ideal gas, Marine Chemistry, 2, 203-215, 10.1016/0304-4203(74)90015-2, 1974.
- 800 Zuijdgeest, A., Baumgartner, S., and Wehrli, B.: Hysteresis effects in organic matter turnover in a tropical floodplain during a flood cycle, Biogeochemistry, 131, 49-63, 10.1007/s10533-016-0263-z, 2016.

https://doi.org/10.5194/egusphere-2025-5756 Preprint. Discussion started: 26 November 2025 © Author(s) 2025. CC BY 4.0 License.





Zurbrügg, R., Wamulume, J., Kamanga, R., Wehrli, B., and Senn, D. B.: River-floodplain exchange and its effects on the fluvial oxygen regime in a large tropical river system (Kafue Flats, Zambia), Journal of Geophysical Research: Biogeosciences, 117, 10.1029/2011jg001853, 2012.